

**БЪЛГАРСКА АКАДЕМИЯ НА НАУКИТЕ**  
**ИНСТИТУТ ПО МИКРОБИОЛОГИЯ**  
**„СТЕФАН АНГЕЛОВ“**



**Eng. Ivanka Kostadinova Koycheva**

**ANTIPSORIATIC ACTIVITY OF PLANT *IN VITRO***  
**SYSTEMS FROM *LAVANDULA ANGUSTIFOLIA* AND**  
***HARPAGOPHYTUM PROCUMBENS*, AND THEIR**  
**BIOLOGICALLY ACTIVE METABOLITES**

**SUMMARY**

**On a dissertation for the award of educational and scientific degree**

**"Doctor" in the field 5.11. Biotechnology**

**(Technology of biologically active substances)**

**Scientific supervisor: Prof. Dr. Milen I. Georgiev**

**Plovdiv, 2025**



**БЪЛГАРСКА АКАДЕМИЯ НА НАУКИТЕ**  
**ИНСТИТУТ ПО МИКРОБИОЛОГИЯ**  
**„СТЕФАН АНГЕЛОВ“**



**Eng. Ivanka Kostadinova Koycheva**

**ANTIPSORIATIC ACTIVITY OF PLANT *IN VITRO***  
**SYSTEMS FROM *LAVANDULA ANGUSTIFOLIA* AND**  
***HARPAGOPHYTUM PROCUMBENS*, AND THEIR**  
**BIOLOGICALLY ACTIVE METABOLITES**

**SUMMARY**

**On a dissertation for the award of educational and scientific degree**

**"Doctor" in the field 5.11. Biotechnology**

**(Technology of biologically active substances)**

**Scientific supervisor: Prof. Dr. Milen I. Georgiev**

**Members of the scientific jury: Prof. Dr. Milka Mileva**

Assoc. Prof. Dr. Petya Dimitrova

Prof. Dr. Velizar Gochev

Assoc. Prof. Dr. Dilyana Nikolova

Assoc. Prof. Dr. Zheni Yordanova

**Plovdiv, 2025**

The dissertation is consisted of 138 pages, 34 figures and 6 tables. The number of literature sources cited are 268.

The dissertation work was approved and scheduled for defense by The National Scientific Seminar on "Applied Microbiology and Microbial Biotechnologies" at the Institute of Microbiology "Stephan Angeloff" – BAS, which session was held on 21.10.2025.

The PhD student was authorised with the right to defend the doctoral thesis by order № I-185/17.12.2024 of the Director of the Institute of Microbiology - BAS, Prof. Dr. Penka Petrova.

The defense of the dissertation will take place on ..... from ..... hours in the seminar hall of the Institute of Microbiology "Stephan Angeloff" – BAS (IMikB), Sofia, Bulgaria.

The materials for the defense are available at IMikB – BAS and are published on the website of IMikB – BAS.

**Content:**

<b>Abbreviations and symbols used .....</b>	<b>4</b>
<b>I. INTRODUCTION .....</b>	<b>6</b>
<b>II. AIM AND OBJECTIVES .....</b>	<b>7</b>
<b>III. MATERIALS AND METHODS .....</b>	<b>8</b>
<b>IV. RESULTS AND DISCUSSION .....</b>	<b>14</b>
1. <i>In vitro</i> determination of the antipsoriatic potential and mechanism of action of a biotechnologically derived extract of <i>L. angustifolia</i> and rosmarinic acid .....	14
2. <i>In vitro</i> determination of the antipsoriatic potential and mechanism of action of a biotechnologically derived extract of <i>H. procumbens</i> , verbascoside and leucosceptoside A .....	24
3. <i>In vivo</i> validation of the anti-inflammatory effect of rosmarinic acid .....	37
4. Conclusion and future perspectives .....	43
<b>V. CONCLUSIONS .....</b>	<b>44</b>
<b>VI. CONTRIBUTIONS .....</b>	<b>45</b>
<b>Acknowledgements .....</b>	<b>46</b>
<b>Published materials on the dissertation .....</b>	<b>47</b>

## Abbreviations and symbols

$\Delta G$	Free energy of binding
AKT	Protein kinase B
CCL	C-C motif chemokine ligand
CD <sub>3</sub> OD	Deuterated methanol
COSY	Homonuclear correlation spectroscopy
CXCL	C-X-C motif chemokine ligand
DEXA	Dexamethasone
DMSO	Dimethyl sulfoxide
HaCaT	Human epidermal keratinocytes
HPLC	High-performance liquid chromatography
HSQC	Heteronuclear single quantum coherence spectroscopy
IFN	Interferon
I $\kappa$ B	NF- $\kappa$ B inhibitory unit
IKK	I $\kappa$ B kinase complex
IL	Interleukin
IMQ	Imiquimod
JAK	Janus Kinase
K <sub>i</sub>	Affinity constant
Ki67	Proliferation marker
LEU	Leucosceptoside A
MAPK	Mitogen activate protein kinase
mRNA	Informational RNA

mTOR	Mechanistic target of rapamycin
MTT	3-(4,5-dimethyl-2-thiazolyl)-2,5-diphenyl-2H-tetrazolium bromide
NF- $\kappa$ B	Nuclear factor kappa B
NMR	Nuclear magnetic resonance
PASI	Psoriasis Area and Severity Index
PI3K	Phosphoinositide 3-kinases
PMA	Phorbol 12-myristate 13-acetate
RA	Rosmarinic acid
RMA	Ribonucleic acid
RT-qPCR	Real-time quantitative reverse transcription polymerase chain reaction
SEM	Standard error of the mean
STAT	Signal transducer and activator of transcription
TCA	Tricarboxylic acids
TOCSY	Total homonuclear correlation spectroscopy
VER	Verbascoside

## I. INTRODUCTION

Psoriasis is a chronic immune-mediated disease with skin and joint manifestations, affecting approximately 2-3% of the world's population. Clinical symptoms mostly include characteristic psoriatic lesions on the skin. Psoriasis is associated with numerous comorbidities such as psoriatic arthritis, obesity, sleep apnea, depression and some autoimmune diseases. The significance of the disease stems from its widespread prevalence, the associated deterioration in patients' quality of life and the corresponding high social burden, which is why psoriasis is recognised by the World Health Organisation as a major non-communicable disease.

Approved medications for the treatment of the disease include retinoids, corticosteroids and several immune-based drugs, which remain the mainstay of treatment. The possibility of drug resistance and the associated adverse effects of conventional antipsoriatic therapy have increased interest in new alternative methods for disease control through the use of natural products. The role of inflammation in this disease suggests that medicinal plants and natural compounds with anti-inflammatory activity may be effective in its treatment. In addition, modulation of inflammatory pathways in keratinocytes may also be one of the directions for an effective therapeutic approach in psoriasis. In the present dissertation, the biological activity of extracts from *in vitro* systems of plant species with known anti-inflammatory activity *Lavandula angustifolia* Mill. (lavender) and *Harpagophytum procumbens* (Burch.) DC. ex Meisn. (devil's claw), as well as their biologically active metabolites was investigated using modern “omics” approaches in an *in vitro* model of psoriasis in human keratinocytes. The molecular mechanisms of their action were also studied. Additionally, the *in vivo* anti-inflammatory potential of rosmarinic acid was validated at the organism level. The decision to analyse biotechnologically derived extracts was carried out in the context of: the limited natural resources and the low content of pharmaceutically significant compounds in wild plant sources; the possibility of obtaining plant material with a relatively constant quantitative and qualitative composition; and the integration of plant *in vitro* systems for the biosynthesis of compounds with high biological value such as rosmarinic acid.

## II. AIM AND OBJECTIVES

### 1. AIM

The aim of the present study is to investigate the pharmacological potential of extracts from *in vitro* cultures of *L. angustifolia* and *H. procumbens*, as well as their biologically active metabolites (rosmarinic acid, verbascoside and leucosceptoside A, respectively) in an *in vitro* model of psoriasis in human keratinocytes, as well as the effect of topical application of rosmarinic acid in an IMQ-induced model of psoriasis in mice.

### 2. OBJECTIVES

- 2.1. Preparation and metabolic profiling of extracts from *in vitro* systems of *L. angustifolia* and *H. procumbens* using nuclear magnetic resonance (NMR).
- 2.2. Isolation of a biologically active compound from extracts *H. procumbens* extracts *in vitro* systems.
- 2.3. Adaptation of an *in vitro* model of psoriatic inflammation by combined cytokine stimulation of human epidermal keratinocyte cell line (HaCaT).
- 2.4. Research of anti-inflammatory activity and molecular mechanism of action of extracts from cell suspensions of *L. angustifolia*, *H. procumbens* and their individual pure compounds in an *in vitro* model of psoriasis in human keratinocytes.
- 2.5. Adaptation of an imiquimod-induced model of psoriasis in mice (C57BL6).
- 2.6. Study of the antipsoriatic potential of rosmarinic acid at the organismal level using an *in vivo* model of psoriasis.



### III. MATERIALS AND METHODS

#### 1. Materials, standards and solvents

Deuterated methanol (CD<sub>3</sub>OD, purity 99.8%) and deuterated water (99.9%) were supplied by Deutero GmbH (Castellaun, Germany). All materials, standards, rosmarinic acid (RA) and solvents used were obtained from Merck KGaA (Darmstadt, Germany). Recombinant human proteins rhIL-17A (#ENZ-PRT188) and rhIL-22 (#ENZ-PRT250) were purchased from Enzo Life Sciences AG (Lausanne, Switzerland), and rhIFN- $\gamma$  (#10067-IF) was obtained from R&D Systems (Minneapolis, Minnesota, USA). The pure compound verbascoside (VER, purity  $\geq$  95%; #4994 S) was supplied by Extrasynthese (Geneille, France). Leucosceptoside A (LEU) was isolated (0.045 g/23.4 g extract, 0.045 g/50 g biomass, respectively) from devil's claw fractions by low-pressure column chromatography (Merck Lobar RP-8 and RP-18 columns), eluting with a water/methanol gradient, as previously described by Georgiev et al. (2010). The ingredients of the formulation for topical application are of pharmacological grade and were supplied by local distributors. Aldara cream (Meda AB, Solna, Sweden) was purchased from the pharmacy chain (Plovdiv, Bulgaria).

##### 1.1. Antibodies

Primary antibodies against AKT (#9272), JAK2 (#3230S), PI3K (#4257), STAT1 (#14994) and phospho-STAT1 (#7649) were supplied by Cell Signaling Technology (Leiden, The Netherlands). Buffers and chemicals for electrophoresis, immunoblot analysis, antibodies against the reference proteins tubulin (#12004166) and  $\beta$ -actin (#AHP2417), and a secondary anti-rabbit IgG antibody Star-Bright Blue 700 (#12004162) were obtained from Bio-Rad Laboratories Inc. (Hercules, CA, USA). Protocols for working with them have been previously described by Vasileva et al. (2020).

#### 2. Methods

##### 2.1. *L. angustifolia* and *H. procumbens* cell suspensions cultivation and extraction

Suspension cultures of lavender and devil's claw were cultured as previously reported on Linsmayer and Skoog liquid medium supplemented with 0.2 mg/L 2,4-dichlorophenoxyacetic acid and 30 g/L sucrose in the dark at 26 °C and with orbital shaking at 110 rpm (Georgiev et al., 2006; Stancheva et al., 2011). After cultivation, the cell suspensions biomass was collected by filtration and the cell material was frozen and lyophilized. Subsequent extraction of the dry biomass was performed with 50% methanol:water under sonication at room temperature for 20 min. The resulting extract was filtered and concentrated by rotary vacuum evaporation at 40 °C (Georgiev et al., 2006; Stancheva et al., 2011). It was subsequently lyophilized and stored at -20 °C before performing chemical analysis and biological tests.

## 2.2. Phytochemical analysis of cell suspension extracts from *L. angustifolia* and *H. procumbens*

### 2.2.1. Nuclear magnetic resonance (NMR) spectroscopy-based metabolic profiling

The NMR analysis was performed according to the protocol described by Georgiev et al. (2015). Proton  $^1\text{H}$  NMR spectra, as well as two-dimensional *J*-resolved, homonuclear (COSY) and heteronuclear (HSQC) correlation spectroscopies, were recorded at 25 °C on a Bruker AVII + 600 spectrometer (Bruker, Karlsruhe, Germany) operating at 600.13 MHz proton frequency with a 4.07 s relaxation time in CD<sub>3</sub>OD.

### 2.2.2. Chromatographic analysis by high-performance liquid chromatography (HPLC)

The quantification of RA in *L. angustifolia* extract and VER and LEU in devil's claw extract was performed using an HPLC system (Waters, Milford, MA, USA) controlled by Breeze software version 3.30 SPA (Waters). The HPLC method was validated for linearity and sensitivity, including limit of detection (LOD) and limit of quantification (LOQ). The RA, VER and LEU contents were determined, according to the protocol used by Choi et al. (2019) with certain modifications and the protocol reported by Georgiev et al. (2011), respectively,.

## 2.3. Cell cultivation and treatment, *in vitro* model of psoriasis

The human epidermal keratinocyte cell line (HaCaT; #330493) was purchased from Cell Line Service GmbH (Eppelheim, Germany). Cell viability of HaCaT was determined by the MTT [3-(4,5-dimethyl-2-thiazolyl)-2,5-diphenyl-2H-tetrazolium bromide; 5 µg/mL] assay. Cells were cultured for 24 hours until confluent. Then incubated with the respective extracts or individual pure compounds, and for each extract and each pure compound with or without stimulation with the cytokine combination interferon (IFN)- $\gamma$ /interleukin (IL)-17A/IL-22 at a concentration of 1/1/1 ng/mL, respectively. The *in vitro* psoriasis model was achieved by exposing HaCaT cells to IFN- $\gamma$ /IL-17A/IL-22 (1 ng/mL each; Slivka et al., 2019) for 1 hour to recreate a psoriasis-like inflammatory environment. Further, keratinocytes were treated with *L. angustifolia* extract (20, 40, 100 µg/mL), or RA (5, 10, 25 µM), or devil's claw extract (20, 40, 100 µg/mL), or VER or LEU (both 5, 10, 20 µM), or dexamethasone (DEXA; 5 µM), or dimethyl sulfoxide (DMSO; 0.2%). The concentration range of the tested extracts and active compounds was determined after evaluating their effect on the HaCaT cell viability. Samples for subsequent biological analyses were collected at 6 and 24 hours after treatment, for isolation of total ribonucleic acid (RNA) and extraction of protein lysates, respectively. Each experiment was performed in at least three replicates.

## 2.4. *In silico* docking analysis

Docking analysis calculations were performed according to the protocol described by Vasileva et al. (2020). The crystal structures of the studied proteins were obtained from the Protein Data Bank, [www.rcsb.org](http://www.rcsb.org), accessed on 01.04.2021, identification codes: 6BBV for JAK2; 1BF5 for phosphorylated STAT1 (pSTAT1), 1O6L for AKT, 5ITD for PI3K.

## 2.5. Immunoblot analysis

Protein lysates were prepared with RIPA buffer supplemented with 1% protease and phosphatase inhibitor cocktail. Total protein concentration was determined using the Bradford method previously described by Vasileva et al. (2020). Equal amounts (50 µg per well) of proteins were separated by vertical electrophoresis and transferred to nitrocellulose membranes, blocked and followed by incubation with primary antibodies against AKT, JAK2, PI3K, STAT1, and p-STAT1. Immunodetection was visualized with a ChemiDoc MP imaging system (Bio-Rad) and the resulting images were analyzed with Image Lab 6.0.1 software (Bio-Rad).

## 2.6. Real-time quantitative polymerase chain reaction (RT-qPCR)

Total RNA from HaCaT cells was isolated with RNeasy® RT reagent and reverse transcribed using the FirstStrand complementary DNA synthesis kit (#PR008) from Canvax (Córdoba, Spain), according to the manufacturer's instructions. GAPDH and TUBB were used as reference genes. Expression of target genes was researched by RT-qPCR using Sso EvaGreen SuperMix (#1725204) on a CFX96 system (Bio-Rad).

## 2.7. Preparation of RA emulsion

For the purpose of the study, a topical formulation was created in the form of an oil-in-water (O/W) emulsion (cream). The formula was developed in six phases (A-E; Table 1). The oil phase (A) and water phase (B) were heated separately under the same conditions. The Phase A was gradually included into the phase B through continuous stirring, followed by cooling the emulsion to 40 °C and phases B, D, E and E were added sequentially. The required amount of RA was incorporated into emulsion to create formulations with a final RA concentration of 0.05, 0.25 and 0.50 %. An identical cream (control) without RA content was also prepared. The emulsion stability and thermal stability of the resulting creams were evaluated according to the BDS 3741:1980 standard.

**Table 1. Rosmarinic acid containing topical formulation composition.**

Фаза	Съставки (INCI)	% w/w
A	Cetearyl alcohol	1.0

	Cetyl alcohol	4.0
	Glyceryl stearate, PEG-100 searate	3.0
	Paraffinum liquidum	4.5
	Stearic acid	1.5
B	Glycerin	1.0
	Tetrasodium EDTA	0.02
	Water	83.58
C	Carbomer	0.2
D	Triethanolamin	0.2
E	Phenoxyethanol, ethylheylglycerin	1.0
F	Rosmarinic acid	q.s.

Legend: q.s. - quantum satis “as much as is enough”; % w/w - percent weight-by-weight.

## 2.8. *In vivo* model of psoriasis

A schematic of the experiment is presented in Figure 1.

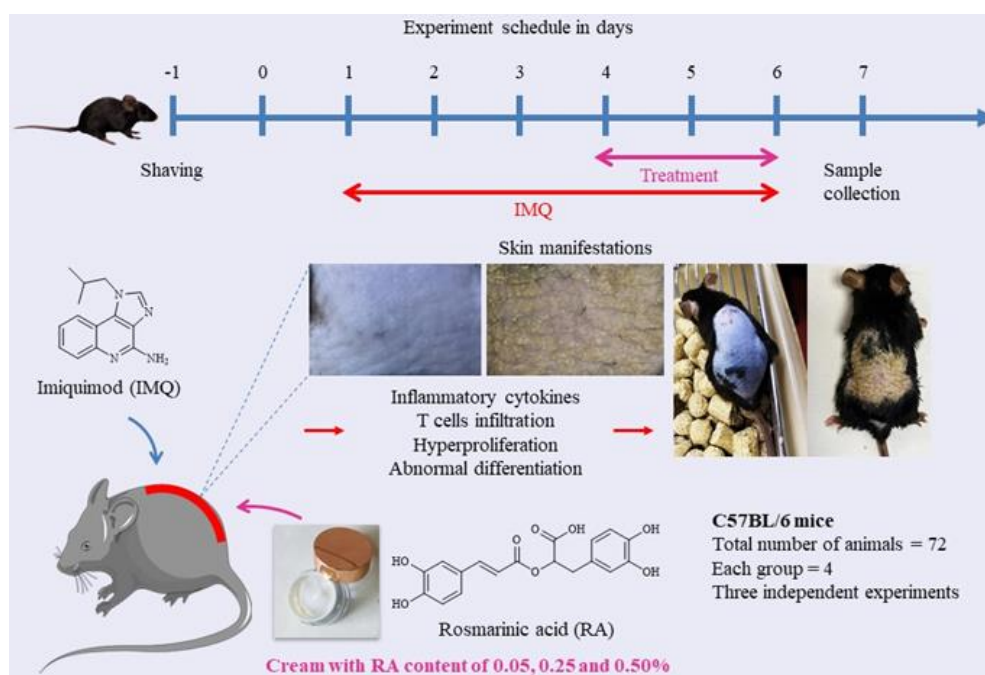


**Figure 1. Experimental design of imiquimod-induced psoriasiform dermatitis.** The psoriasis model was induced on the hairless back skin of C57BL/6 mice by daily topical application of imiquimod (IMQ) for 6 consecutive days. The animals were grouped into six experimental categories: healthy control, IMQ, IMQ+0.05% RA, IMQ+0.25% RA and IMQ+0.5% RA, IMQ+0.05% betamethasone. The back skin of all mice was shaved and one day later a IMQ cream was applied for six consecutive days, except for the animals in the healthy control group (Healthy

mice), which were treated with a cream without RA. From day 4, cream containing RA (0, 0.05, 0.25 and 0.50%) was applied topically in the respective experimental groups 1 hour before the application of the IMQ cream.

The C57BL/6 mice (male, 8-12 weeks old; purchased from Jackson Laboratory, CT, USA) were used to establish a model of psoriatic dermatitis. The *in vivo* model was achieved by daily topical application of 62.5 mg of Aldara cream, which contains 5% IMQ, delivering a dose of the active compound of approximately 3 mg/mouse/day to a hairless area of skin on the back of the animals - 2.0 cm<sup>2</sup> (van der Fits et al., 2009; Gangwar et al., 2022; Köhler et al., 2024). A cream containing 0.05% betamethasone dipropionate (betamethasone; Merck Sharp and Dome Bulgaria EOOD, Sofia, Bulgaria) was used as a positive control in this experiment. The animals were randomly assigned with four animals per group. Three independent experiments were performed - a total of 10-12 animals per group.

The experimental procedures were carried out in the vivarium of the Stephan Angeloff Institute of Microbiology-BAS, Sofia (Registration - Protocol 352/06.01.2012, reg. No. 11130005). The animals were maintained under specific pathogen-free conditions, with controlled temperature and *ad libitum* access to water and food. The animal experiments were conducted under veterinary control and in accordance with national legislation (SG No. 87 of 2006) and Decree No. 20 of 01.11.2012, the European Animal Protection Directive (2010/63/EU) and the animal research: reporting of *in vivo* experiments guidelines (AR-RIVE). A permit No. 331 (valid until 07.06.2027) was issued by the Bulgarian Food Safety Agency for the planned experiments.

## 2.9. Psoriasis Area and Severity Index (PASI) assessment

The severity of psoriasis was assessed using the PASI index, which is based on a scoring system that considers changes in skin color (erythema), scaling, and thickness compared to healthy skin. A 0-4 rating scale was used: 0-no change; 1-minor change; 2-moderate change; 3-significant change; 4-severe change. The severity of psoriatic inflammation was determined by the cumulative score (erythema + scaling + thickening) on the van der Fits scale of 0-12 (van der Fits et al., 2009). The weight of the animals was recorded every two days, along with changes in skin thickness, redness, and scaling. At the end of the experiment (day 7), the animals were sacrificed by cervical dislocation and their spleens, inguinal, and axillary lymph nodes were dissected and weighed.

## 2.10. Isolation of murine T-cells from spleen and cell proliferation analysis

Spleens from healthy C57BL/6 mice were dissected and a single cell suspension was prepared. The

T-lymphocytes were then magnetically separated from the resulting cell suspensions using negative selection (MS T Lymphocyte Enrichment IMAG DM Set; BD Bioscience, Heidelberg, Germany) according to the manufacturer's recommendations. Purified T-cells ( $2 \times 10^6$  cells/mL) were incubated in the presence of RA (1, 5, 25  $\mu$ M) for 24 and 48 h at 37 °C, 5% CO<sub>2</sub>. Cells were also incubated with: phorbol 12-myristate 13-acetate (PMA; 50 ng/mL), PMA/ion group and DEXA (50 ng/mL/750 ng/mL and DEXA, 5  $\mu$ M), DEXA (5  $\mu$ M), DEXA and RA (5  $\mu$ M and 25  $\mu$ M), 0.05% DMSO or without any additional substances (control group). The T-cell proliferation assay was performed with MTT reagent (5 mg/mL) as previously described by Boneva et al (2023).

#### 2.11. Histological evaluation of psoriatic skin lesions

The skin treated area of the experimental animals was separated and biopsies were taken. The skin samples (6 mm) were fixed in 10% buffered formalin pH 7.0. After washing, the test material was prepared for embedding in paraffin by dehydration with increasing alcohol concentration (45 min in 70% ethanol solution; 45 min in 80% ethanol solution; 45 min in 95% ethanol solution; 2x60 min in pure 100% ethanol; 2x60 min in xylene substitute; 3x60 min in liquid paraffin at 58 °C) in an automatic tissue processor from Leica Biosystems (Nussloch, Germany). Then, 5-7  $\mu$ m thick histological sections were obtained from the paraffin blocks with the analyzed tissues using a Leica RM2125 RTS manual rotary microtome (Leica Biosystems, Wetzlar, Germany). The obtained preparations were deparaffinized and stained with hematoxylin and eosin. To determine the thickness of the epidermis of each sample, an algorithm was used using the ImageJ software to calculate the area of the epidermis divided by its length (Jabeen et al., 2020).

#### 2.12. Statistical analysis

Statistical evaluation of the data obtained from the *in vitro* experiments was performed using SigmaPlot v11.0 software (Systat Software GmbH, Erkrath, Germany) and the data are presented as mean  $\pm$  standard error of the mean (SEM). Differences between groups were determined by unpaired Student' t-test as appropriate or one-way analysis of variances (ANOVA) with Bonferroni's post hoc test when more than two groups were compared. The data obtained from the *in vivo* experiments were evaluated using GraphPad Prism software (San Diego, CA, USA). For statistical comparison of more than two groups and for multivariate analyses, the one-way ANOVA test was used, followed by Dunnett's test for pairwise comparisons or Tukey's test for multiple comparisons. A difference of p values < 0.05 was considered statistically significant.



## IV. RESULTS AND DISCUSSION

The experimental approach summarized in Figure 2 was used to achieve the goal of this dissertation.

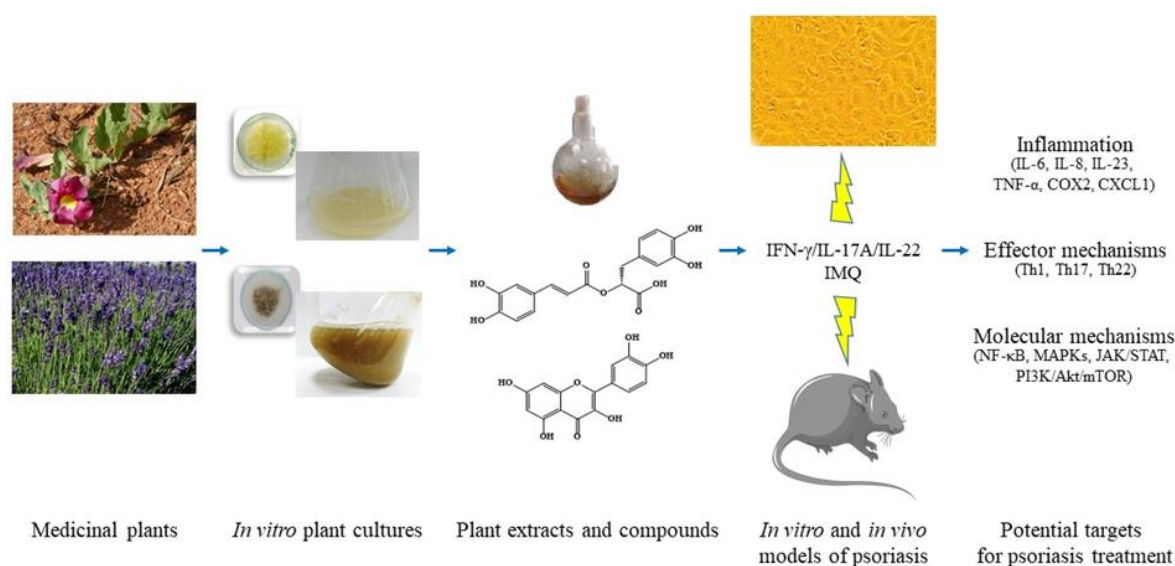


**Figure 2. Experimental strategy to establish the mechanisms of modulation of inflammation in psoriasis by applying plant extracts and individual pure compounds.**

### 1. Chemical characterization and *in vitro* determination of the antipsoriatic potential and mechanism of action of a biotechnologically derived extract of *L. angustifolia* and RA

The therapeutic potential of *L. angustifolia* extract and RA was evaluated by studying their biological activity in cytokines IFN-γ/IL-17A/IL-22-induced psoriasis-like inflammation model in human keratinocytes.

#### 1.1. Phytochemical characterization of a biotechnologically derived extract of *L. angustifolia*

Metabolic profiling by NMR has great potential for the study of various biological systems. In the present study, the *L. angustifolia* cell suspension extract was subjected to phytochemical analyses to confirm the presence of RA in it (Table 2).

**Table 2. Chemical shifts ( $\delta$ ) and coupling constants ( $J$ ) of metabolites, identified by analysis of  $^1\text{H}$  NMR spectra of *L. angustifolia* extract (Pereira et al., 2013, Georgiev et al., 2015 and Marchev et al., 2017).**

Metabolite	Chemical shift (ppm)	Coupling constant (Hz)
$\alpha$ -Glucose	5.19	(d, $J = 3.7$ )
$\beta$ -Glucose	4.59	(d, $J = 7.9$ )

	1.92/2.30/3.01	(m)/(t, $J = 7.2$ )/(t, $J = 7.3$ )
$\gamma$ -Aminobutyric acid		
Alanine	1.49	(d, $J = 7.3$ )
Valine	1.01/1.06	(d, $J = 7.1$ )/(d, $J = 7.1$ )
Glutamate	2.37/2.06	(m)/(m)
Glutamine	2.14/2.37	(m)/(m)
Sucrose	5.41/4.18	(d, $J = 3.9$ )/(d, $J = 8.9$ )
Inosine	8.24/8.35	(s)/(s)
Inositol	3.95/3.52/3.21	(m)/(m)/(m)
Formic acid	8.48	(s)
Acetic acid	1.91	(s)
Pyruvic acid	2.43	(s)
Rosmarinic acid	7.12/6.88/7.04/7.52/6.32/6.84 /6.78/6.72/2.94/3.1/ 5.03	(d, $J = 2.1$ )/(d, $J = 8.2$ )/(dd, $J = 8.4$ , 2.1)/(d, $J = 15.9$ )/(d, $J = 15.9$ )/(d, $J =$ 2.0)/(d, $J = 8.1$ )/(dd, $J = 8.1$ , 2.0)/(dd, $J = 14.4$ , 10.0)/(dd, $J = 14.5$ , 3.5)/(dd, $J = 10.0$ , 3.4)
Threonine	1.33	(d, $J = 6.8$ )
Fumaric acid	6.53	(s)
Choline	3.22	(s)

According to the  $^1\text{H}$  NMR spectrum data, the signals with the highest intensity in the aromatic region corresponded to the characteristic signals of RA, confirming the presence of this phenolic acid as the main secondary metabolite in the extract. In the aliphatic region ( $\delta$  0.5-3.0 ppm) signals were detected for the organic acetic and pyruvic acids, and in the region  $\delta$  6.5-8.5 ppm signals for formic and fumaric acids were also present. The identified metabolites are important intermediates of the tricarboxylic acid (TCA) cycle, in which compounds identified in the carbohydrate region ( $\delta$  3.0-5.5), such as  $\alpha$ -glucose,  $\beta$ -glucose and sucrose, are oxidized to form pyruvate. The TCA cycle initiates pathways that lead to important structural metabolites, including the amino acids alanine, glutamine, glutamate, threonine and valine, identified in the extract (Table 2).

In addition to the proton NMR spectra obtained, RA was structurally identified by 2D NMR spectra, which provide more complete and accurate information about the structures contained in the extract (Figure 3). The presence of RA in the analyzed extract was confirmed by the interactions through a single proton-carbon bond (cross-peaks) observed in the HSQC spectrum (Figure 3A).



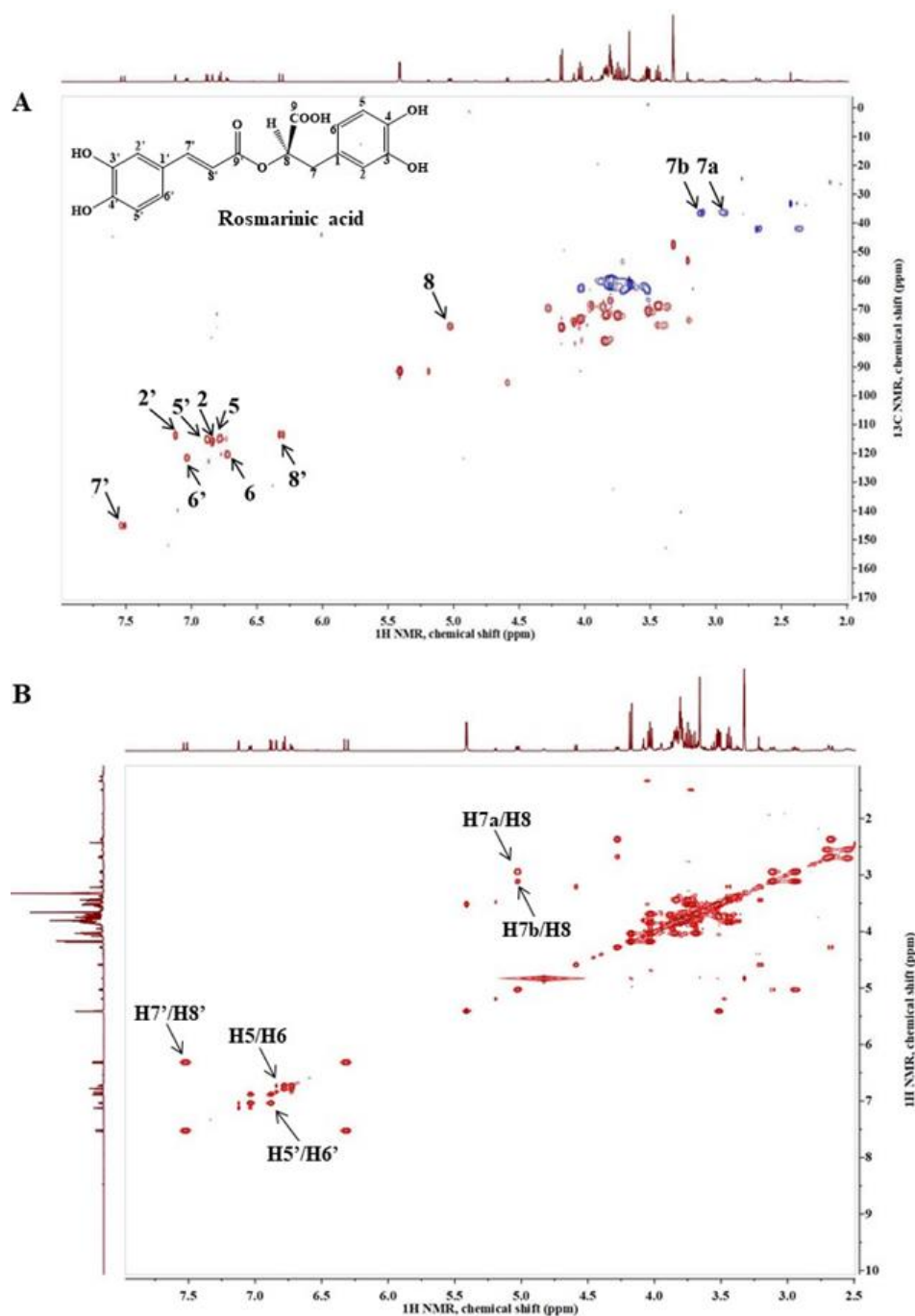


**Figure 3. NMR spectra of *L. angustifolia* cell suspension extract and characteristic signals of rosmarinic acid (RA). Heteronuclear single quantum coherence spectroscopy (<sup>1</sup>H-<sup>13</sup>C HSQC; A) and homonuclear correlation spectroscopy (<sup>1</sup>H-<sup>1</sup>H COSY; B).**

The spectra of the extract revealed the content of overlapping signals between the doublet at  $\delta_H$  7.52 and a carbon atom signal at  $\delta_C$  145.14, as well as between the doublet at  $\delta_H$  6.32 and  $\delta_C$  113.36. The two doublets were assigned to a pair of trans-olefin protons (H-7' and H-8') based on the large coupling constant ( $J = 15.9$  Hz) observed in the <sup>1</sup>H NMR spectrum, indicating the presence

of a *trans*-caffeoyl residue in the molecule. Furthermore, the ABX system of caffeic acid was confirmed by the overlapping peaks observed among the signals for the three aromatic protons H-5', H-6' and H-2' and the corresponding carbon atoms at  $\delta_H$  6.88/ $\delta_C$  115.21,  $\delta_H$  7.04/ $\delta_C$  121.59 and  $\delta_H$  7.12/ $\delta_C$  113.84, respectively. The other ABX system in the aromatic region is assigned to the 3,4-dihydroxyphenyl residue, according to the peak overlaps between the signals for the three protons H-5, H-6 and H-2 and the corresponding carbon atoms observed at  $\delta_H$  6.78/ $\delta_C$  114.87,  $\delta_H$  6.72/ $\delta_C$  120.61 and  $\delta_H$  6.84/ $\delta_C$  116.02. The doublet at  $\delta_H$  5.03, correlated with the carbon atom signal at  $\delta_C$  75.84, suggests the presence of a CH group bonded to an oxygen atom, and this signal is assigned to H-8. Two doublets at  $\delta_H$  2.94 and 3.11 have peak overlaps with a signal for a single carbon atom  $\delta_C$  36.36, which is indicative of the presence of a methylene group at position 7. In addition,  $^1H$ - $^1H$  COSY interactions are shown in Figure 3B. The detected cross-peaks between H-7'/H-8' ( $\delta_H$  7.52/  $\delta_H$  6.32), H6'/H-5' ( $\delta_H$  7.04/ $\delta_H$  6.88) and H6/H-5 ( $\delta_H$  6.72/ $\delta_H$  6.78) confirmed the structure of RA. The data are in agreement with those in the literature (Xiao et al., 2008; Pereira et al., 2013; Zhao et al., 2021). Additionally, the content of RA in the analyzed extract was determined by HPLC –  $100.16 \pm 7.01$  mg/g dry extract (Figure 4). The HPLC method was validated for linearity and sensitivity in the concentration range between 10 and 200  $\mu$ g/mL. The LOD and LOQ values were 6.9 and 14.59  $\mu$ g/mL, respectively.

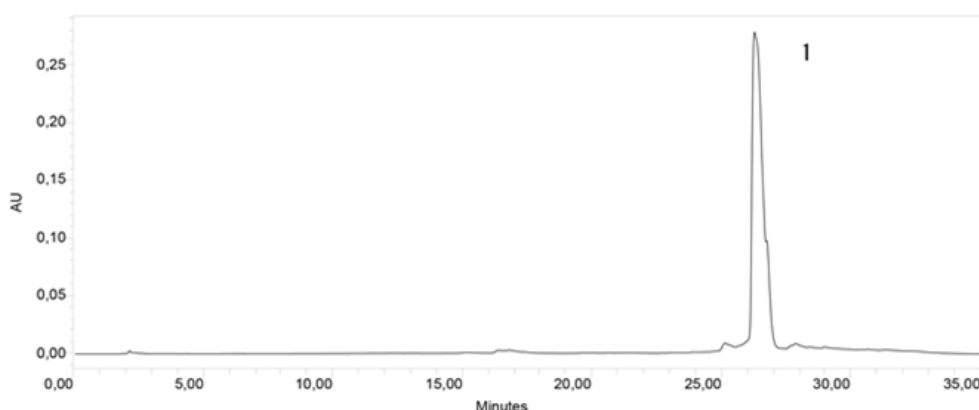


**Figure 4.** HPLC chromatogram of *L. angustifolia* cell suspension extract. Peak 1: rosmarinic acid.

### 1.2. *In vitro* evaluation of the antipsoriatic potential of *L. angustifolia* and RA

Little is known about the role of RA in keratinocyte physiology. RA has previously been reported to counteract UVA-induced damage in murine melanoma cells (Sanchez-Campillo et al., 2009), and inhibit IFN- $\gamma$ -induced inflammation in primary human keratinocytes (Georgiev et al., 2012). As a starting point, the development of HaCaT was studied. Figure 5 shows the growth curve of keratinocytes at 24, 48 and 72 hours.

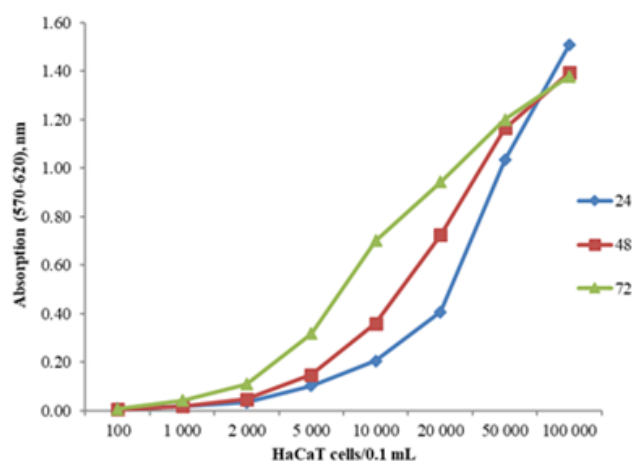


**Figure 5. Growth dynamics of the HaCaT keratinocyte cell line.**

### 1.2.1. Determination of non-toxic treatment concentrations

A cell viability assay was performed on HaCaT to determine the effect of treatment with different concentrations of the biotechnologically derived *L. angustifolia* extract and RA. The 24 hours exposure of the extract and RA did not significantly affect HaCaT cell viability up to 100 µg/mL for the extract and 100 µM for RA, respectively (Figure 6).

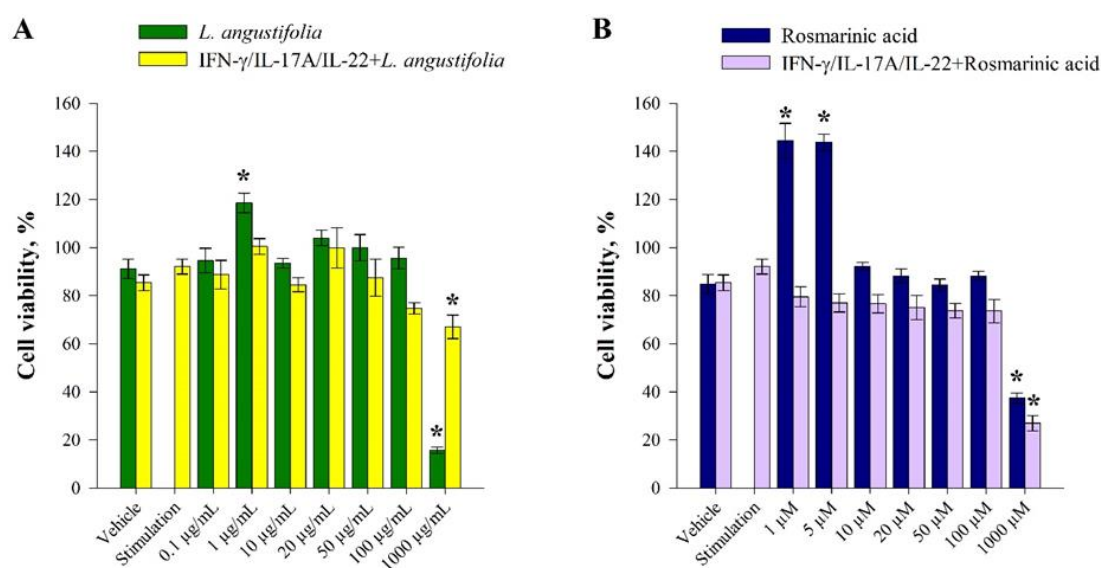


**Figure 6. Effect of *L. angustifolia* cell suspension extract (A) and pure rosmarinic acid (B) on cell viability of human keratinocytes.** Neither *L. angustifolia* nor RA significantly affected the viability of HaCaT cells at 24 h of treatment. The results are expressed of three independent experiments (mean ± SEM, \*p<0.05 compared to untreated controls).

### 1.2.2. *Lavandula angustifolia* extract and rosmarinic acid reduce psoriasis-associated inflammatory changes in gene expression profile in human keratinocytes

The interaction between activated immune cells and keratinocytes is a key factor in the pathology of psoriasis. Therefore, inflammatory cytokines induce a psoriatic phenotype in keratinocytes (Federici et al., 2002; Nograles et al., 2008; Nestle et al., 2009; Greb et al., 2016). In this research, stimulation with the combination of inflammatory cytokines IFN- $\gamma$ /IL-17A/IL-22 induced changes in the messenger RNA (mRNA) expression profile of human keratinocytes that mimicked a psoriasis-like transcriptional signature (Figure 7).

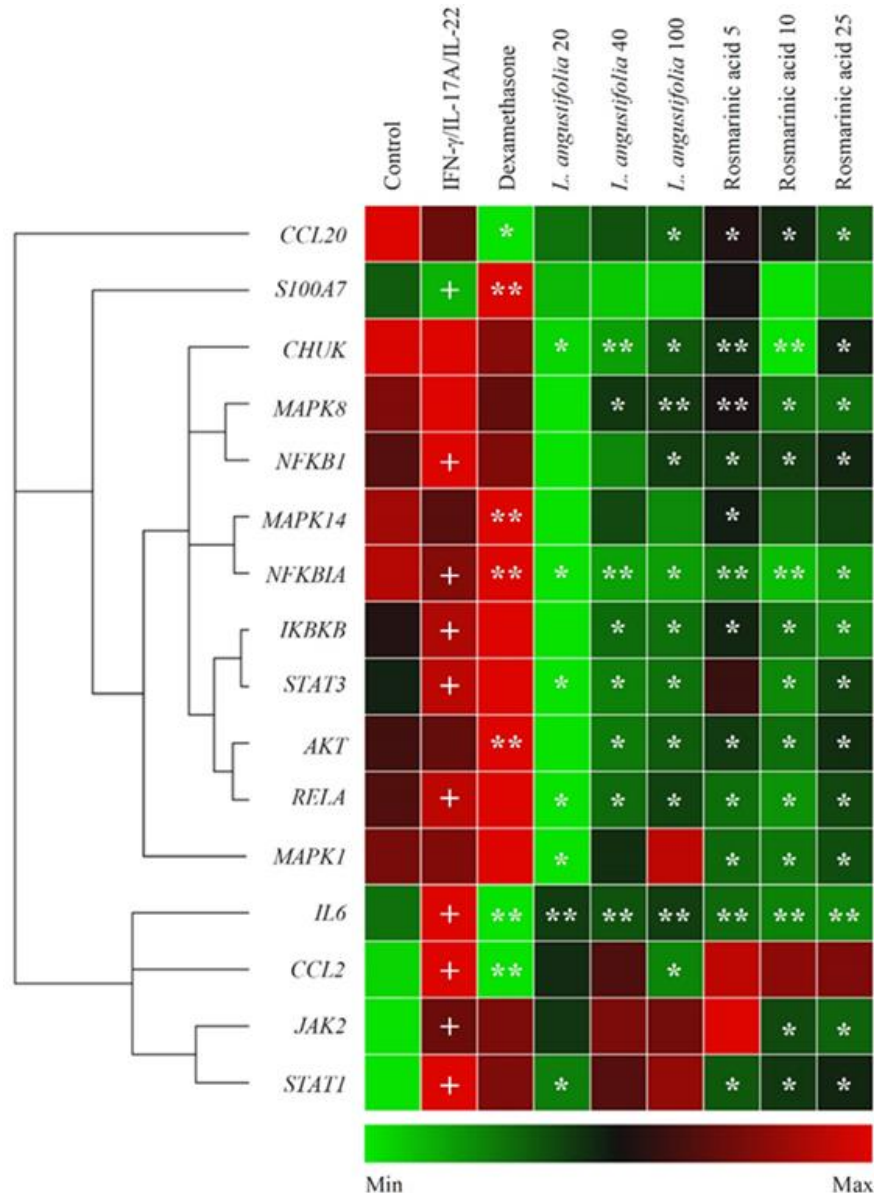


**Figure 7. *L. angustifolia* extract and rosmarinic acid down-regulate the expression of inflammation-related genes in psoriasis-like model in human keratinocytes.** Clustergram and heatmap from relative gene expression analysis by RT-qPCR. The results are expressed from three independent experiments (mean  $\pm$  SEM; +p < 0.05 compared to control cells; \*p < 0.05 and \*\*p < 0.01 compared to model group).

Chronic inflammation, abnormal proliferation and differentiation of keratinocytes are significant events associated with the development of psoriasis (Girolomoni et al., 20017; Albanesi et al., 2018). Consequently, inhibition of keratinocyte inflammation may be an effective therapeutic approach in the psoriasis treatment. Activated keratinocytes respond to immune stimulation in an attempt to counteract psoriatic changes by secreting chemoattractant molecules, such as MCP1 and (C-C motif ligand) CCL20, inflammatory cytokines (IL-6, IL-8, IL-4) and antibacterial peptides (S100A; Wolk et al., 2006; Nograles et al., 2008; Andres et al., 2013; Greb et al., 2016; Lee et al., 2019; Liang et al., 2019). However, induced inflammatory factors further attract immune cells to psoriatic lesions and deteriorate the inflammatory environment (Wolk et al., 2006; Nograles et al., 2008; Wolf et al., 2010; Itoh et al., 2019). Exposure of keratinocytes to the cytokine combination IFN- $\gamma$ /IL-17A/IL-22 represents a reliable model of psoriatic inflammation *in vitro* (Kim et al., 2014; An et al., 2018; Kim et al., 2018; Shi et al., 2018; Zhang et al., 2018; Slivka et al., 2019; Li et al., 2020). As expected, stimulation of keratinocytes with IFN- $\gamma$ /IL-17A/IL-22 in the present study resulted in high expression levels of the inflammatory factors *IL-6* and *CCL2* (encoding MCP1), confirming the induction of psoriatic inflammation. Application of the *L. angustifolia* extract dose-dependently reversed the direction of the upregulation of *IL-6*, *CCL2*, and *CCL20*. Similarly, treatment with RA, at concentrations corresponding to the doses found in the extract, further reduced *IL-6* expression to levels comparable with DEXA treatment.

The psoriatic condition is also characterized by activation of inflammatory signaling pathways. The nuclear factor kappa B (NF- $\kappa$ B) pathway is a key regulatory pathway during inflammation and is considered as a crucial mediator in the pathogenesis of psoriasis (Andres et al., 2013; Kim et al., 2014; Zhang et al., 2018). In the present study, key genes responsible for NF- $\kappa$ B activation were investigated, namely: *CHUK*, *IKBKB*, *NFKBIA*, *NFKB1* and *RELA*. Stimulation of HaCaT cells with the combination of cytokines led to an increase in their expression. Glucocorticoid therapy, frequently applied in psoriasis, acts primarily through inhibition of NF- $\kappa$ B in order to exert its potent anti-inflammatory effect (Bigas et al., 2018). Therefore, DEXA treatment expectedly showed downregulation of the expression of NF- $\kappa$ B downstream targets such as *IL-6*, *CCL2* and *CCL20*. Treatment with both *L. angustifolia* extract and RA downregulated all the examined NF- $\kappa$ B pathway genes. Furthermore, the inhibition of their expression by the extract at the highest concentration (100  $\mu$ g/mL) exceeded that achieved by DEXA. The RA treatment also showed a dose-dependent decrease, which was more effective than that achieved by DEXA but not by the extract. These results suggest that RA is only partially responsible for the inhibition of NF- $\kappa$ B-related genes achieved by *L. angustifolia* extract. Hierarchical cluster analysis of relative gene expression data obtained by RT-qPCR furthermore revealed significant upregulation of Janus

kinase (JAK)/signal transducer and activator of transcription (STAT)-related genes (Shi et al., 2011; Schwartz et al., 2017; Sun et al., 2019), mitogen-activated protein kinase (MAPK) p38/protein kinase B (AKT) signaling pathways, as well as proinflammatory cytokines. In agreement with previous reports using similar combinatorial stimulation to model psoriasis in keratinocytes, overexpression of *JAK2*, *STAT1*, and *STAT3* genes was found (Kim et al., 2014; An et al., 2018; Zhang et al., 2018; Li et al., 2020). In the present experiment, the increase in *STAT1* gene expression was about 10-fold higher than the overexpression of *STAT3* upon IFN- $\gamma$ /IL-17A/IL-22 stimulation, indicating *STAT1* as being more strongly affected in the this model.

The strong effect of the extract on NF- $\kappa$ B genes suggests its potent anti-inflammatory effect in psoriatic keratinocytes. Supporting this is the fact that the key genes *STAT3*, *AKT* and *MAPK8* (encoding the JNK protein) were significantly inhibited upon application of the *L. angustifolia* extract. This suggests that the extract suppresses the relevant JAK/STAT, MAPK and phosphatidylinositol 3-kinase (PI3K)/AKT signaling pathways. Similar to the treatment with the *L. angustifolia* extract, the gene expression of *STAT3* and *AKT* was also affected by RA, but to a lesser extent. Moreover, the expression of the *MAPK8* and *MAPK1* (encoding ERK1/2 protein) was dose-dependently decreased as a result of RA administration. Interestingly, RA treatment of stimulated keratinocytes resulted in significant suppression of *JAK2* and *STAT1*, which was not observed with the extract treatment. All these results indicate that *L. angustifolia* extract mainly affects genes of NF- $\kappa$ B signaling in activated keratinocytes, while RA also suppresses JAK/STAT signaling. The data of the RT-qPCR gene expression analysis clearly demonstrate that lavender extract and RA significantly and concentration-dependently suppress the expression of almost all the studied genes (pro-inflammatory and/or psoriasis-specific). Therefore, psoriasis-related inflammation in keratinocytes can be suppressed by treatment with *L. angustifolia* extract and RA.

### 1.2.3. *Lavandula angustifolia* extract and RA suppress JAK2/STAT1 signaling in human keratinocytes

Immunoblot data indicate that *L. angustifolia* extract and pure RA disrupt JAK2/STAT1 signaling in keratinocytes. Cytokines such as IFN- $\gamma$ , IL-17A, or IL-22 bind to cell surface receptors and signal transduction occurs through JAKs, which in turn promotes phosphorylation and activation of STAT1 and/or STAT3 in psoriasis (Kim et al., 2014; Zhang et al., 2018; Itoh et al., 2019). Increased levels of pSTAT1 have been found in psoriatic lesions (Antunes et al., 2011; Hald et al., 2013). Since in the present study, *STAT1* gene expression was preferentially activated over *STAT3* as a result of cytokine stimulation, the ability of RA to counteract STAT1 activation at the protein level was also assessed (Figure 8).



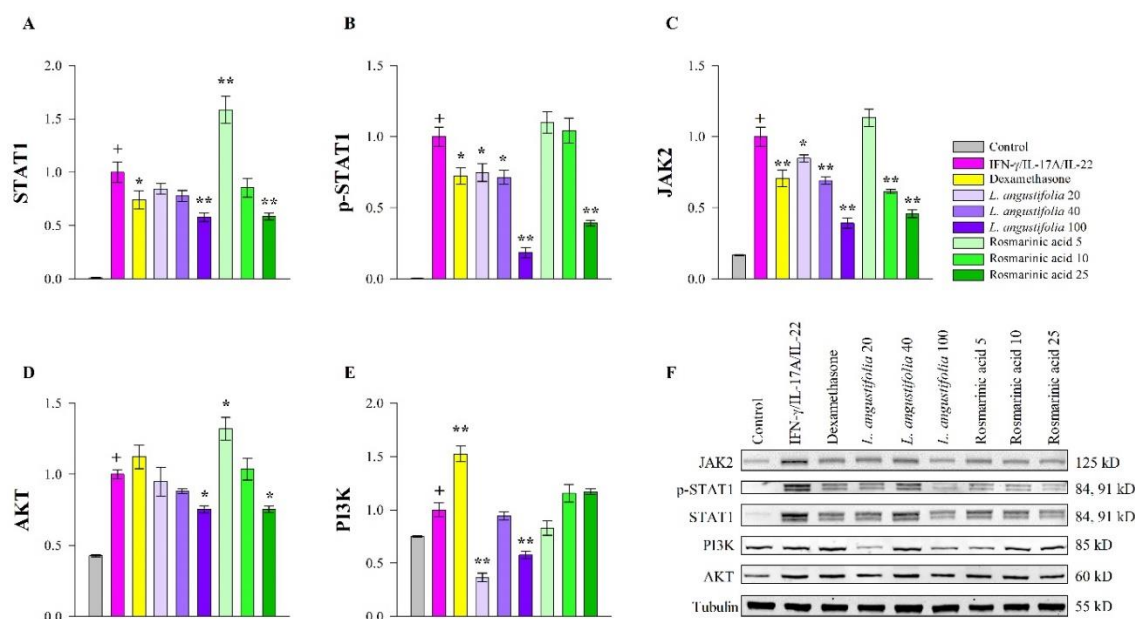


**Figure 8. *L. angustifolia* extract and pure rosmarinic acid both inhibit JAK2/STAT1 signaling in HaCaT cells.** Protein expression of STAT1 (A), phosphorylated STAT1 (B), JAK2 (C), AKT (D), PI3K (E) and representative blots from immunoblot analysis (F), normalized to tubulin. The results are presented of three independent experiments (mean  $\pm$  SEM; +p < 0.05 compared to control cells; \*p < 0.05 and \*\*p < 0.01 compared to model group).

Immunoblot analysis showed that the inhibitory effects of both the extract and RA on total STAT1 (Figure 8A) and pSTAT1 levels (Figure 8B) in HaCaT were dependent on the treatment concentrations. Furthermore, at the highest concentration used, the reduction in STAT1 and pSTAT1 levels was greater than that achieved by DEXA. Also, lavender extract and RA significantly reduced JAK2 protein levels (Figure 8B) in a concentration-dependent manner. This suggests that the inhibition of STAT1 activation is achieved through JAK2 suppression. The RT-qPCR analysis showed that the transcriptional activity of *JAK2* and *STAT1* was significantly reduced by RA (Figure 7), which is consistent with the observed changes at the protein level. The results indicate that STAT1 emerges as a key target of both *L. angustifolia* extract and RA, through which they exert their anti-inflammatory effect in psoriatic keratinocytes. The present study provides evidence that the extract and RA both effectively restore STAT1 phosphorylation to levels exceeding those of DEXA. This suggests that RA may block STAT1 signaling in keratinocytes.

The involvement of PI3K/AKT signaling in cell proliferation is a hallmark of psoriasis in terms of hyperkeratinization (Engelman et al., 2006; Li et al., 2019b; Thatikonda et al., 2020). Gene expression analysis data revealed that *L. angustifolia* extract and RA both downregulated AKT (Figure 7) to a similar extent as DEXA treatment. To further elucidate the mechanism of the extract

and RA inhibition of psoriasis in activated keratinocytes, the PI3K/AKT signaling pathway was also investigated at the protein level. Treatment with their highest concentrations, 100 µg/mL for the extract and 25 µM for RA, respectively, resulted in a decrease in AKT protein levels (Figure 8D), while PI3K (Figure 8E) was only affected by *L. angustifolia* extract. Based on the above, it is suggested that the interaction of the extract with PI3K/AKT signaling may be due to the phytochemical complexity of the extract. The modulation of PI3K/AKT observed upon treatment with *L. angustifolia* extract deserves further investigation, as it may lead to reduced proliferation of psoriatic keratinocytes and consequently reduce lesion size.

Based on the results obtained, a molecular mechanism of biological action of *L. angustifolia* extract and pure RA in an in vitro model of psoriasis was proposed (Figure 9).

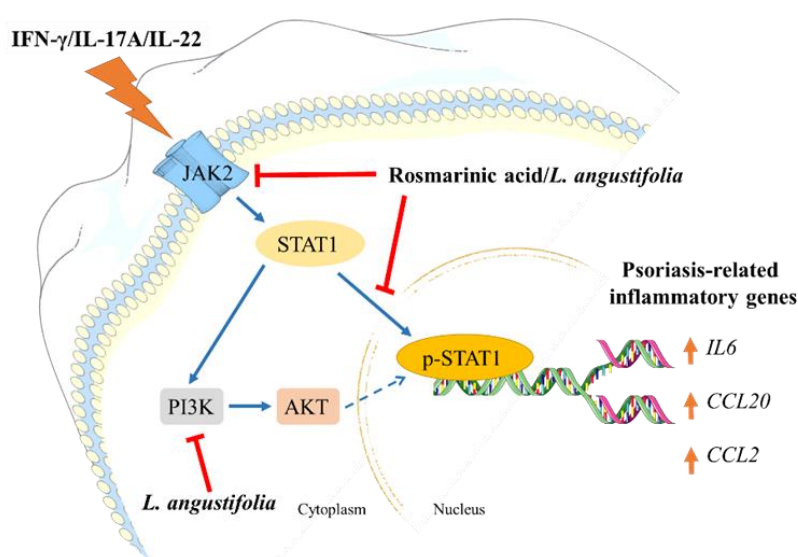


**Figure 9. Schematic representation of the proposed mechanisms of action of *L. angustifolia* extract and rosmarinic acid in psoriasis-like inflammation model in human keratinocytes.** HaCaT cells exposed to the combination of IFN-γ/IL-17A/IL-22 stimuli respond with activation of the JAK2/STAT1 and PI3K/AKT signaling pathways. Activation of JAK2 upon cytokine stimulation leads to activation of STAT1 and its subsequent phosphorylation. After nuclear translocation phosphorylated STAT1 induces transcriptional activation of psoriasis-related inflammatory genes (*IL6*, *CCL20*, *CCL2*). The activated PI3K/AKT axis in psoriatic keratinocytes correlates with induction of hyperproliferation and worsening of the inflammatory milieu. In the present study, both RA and *L. angustifolia* extract inhibited JAK2 and reduced STAT1 phosphorylation, preventing activation of the inflammatory process. Furthermore, *L. angustifolia* extract disrupted PI3K/AKT signaling, which may contribute to reduced proliferation in activated keratinocytes. Taken together, the obtained results suggest an inhibitory effect of *L. angustifolia* extract and RA on psoriasis-related inflammation in human keratinocytes.



Since RA has been shown to be relatively safe for normal cells in most laboratory studies (Domitrovic et al., 2014; Liang et al., 2016; Shang et al., 2016; Nunes et al., 2017; Chen et al., 2018; Joardar et al., 2019; Leu et al., 2019; Luo et al., 2020; Vasileva et al., 2021), the results obtained in this study suggest that RA can be applied as a potential therapy to combat psoriasis. The moderate bioavailability of RA when administered orally is usually a disadvantage for its use in drug therapy (Nunes et al., 2017; Shen et al., 2017; Luo et al., 2020). On the other hand, topical application of RA has been found to be effective in skin disease models, such as atopic dermatitis mouse model (Jang et al., 2011). Most preferably, antipsoriatic preparations are used topically, so that RA and RA-rich extracts such as *L. angustifolia* extract can be successfully integrated into products (ointments, gels, creams) for the treatment of psoriasis.

In summary, the results obtained indicate that the biotechnologically produced *L. angustifolia* extract reduces psoriatic inflammation in human keratinocytes by interfering with JAK2/STAT1 signaling and its efficacy is due to the content of RA. Furthermore, both the extract and RA regulate NF- $\kappa$ B-related genes. It is also clear that the extract can affect PI3K/AKT signaling, suggesting a potential modulation of keratinocyte proliferation in psoriasis (Figure 8). Overall, these results suggest that the biotechnologically produced *L. angustifolia* extract or RA may find application as promising therapeutic alternatives in the treatment of psoriasis. Further *in vivo* validation is needed to confirm their efficacy in psoriatic therapy.

## 2. Chemical characterization and *in vitro* determination of the antipsoriatic potential and mechanism of action of a biotechnologically derived extract of *H. procumbens*, verbascoside and leucosceptoside A

The biological activity and molecular mechanisms of action of *H. procumbens* extract and VER and LEU was investigated in an *in vitro* psoriasis model in human keratinocytes.

### 2.1. Phytochemical characterization of *H. procumbens* extract

Metabolic profiling of the devil's claw extract was achieved by NMR, and primary metabolites were identified along with phenylethanoids VER and LEU (Table 3).

**Table 3. Chemical shift ( $\delta$ ) and coupling constant ( $J$ ) of metabolites identified by analysis of  $^1\text{H}$  NMR spectra of *H. procumbens* cell suspension extract (Georgiev et al., 2011; Santos-Cruz et al., 2012; Youssef et al., 2017; Burgos et al., 2020).**

Metabolite	Chemical shift (ppm)	Coupling constant (Hz)
$\alpha$ - Glucose	5.19	(d, $J = 3.8$ )

$\beta$ - Glucose	4.59	(d, $J = 7.9$ )
Alanine	1.49	(d, $J = 7.2$ )
Valine	1.01/1.06	(d, $J = 7.3$ )/(d, $J = 7.1$ )
Verbascoside	1.06/2.84/4.08/3.97/4.49/5.13/ 6.37/6.69/6.79/6.80/6.89/7.08/ 7.16/7.66	(d, $J = 7.2$ )/(m)/(m)/(m)/(d, $J = 7.9$ )/(d, $J = 1.6$ )/(d, $J = 16.0$ )/(dd, $J = 8.1$ ; 2.0)/(d, $J = 8.6$ )/(d, $J = 2.0$ )/(d, $J = 8.3$ )/(dd, $J = 8.4$ ; 2.1)/(d, $J = 2.0$ )/(d, $J = 16.0$ )
Glutamine	2.14/2.38	(m)/(m)
Sucrose	5.41	(d, $J = 3.9$ )
Leucosceptoside A	1.06/2.84/4.08/3.97/4.49/5.13/ 6.44/6.69/6.79/6.80/6.91/7.15/ 7.26/7.72	(d, $J = 7.2$ )/(m)/(m)/(m)/(d, $J = 7.9$ )/(d, $J = 1.6$ )/(d, $J = 16.2$ )/(dd, $J = 8.1$ ; 2.0)/(d, $J = 8.6$ )/(d, $J = 2.0$ )/(d, $J = 8.4$ )/(dd, $J = 8.2$ ; 1.7)/(d, $J = 2.0$ )/(d, $J = 15.6$ )
Formic acid	8.47	(s)
Acetic acid	1.92	(s)
Serine	3.94	(m)
Threonine	1.33	(d, $J = 6.3$ )
Fructose	4.18	(d, $J = 8.6$ )
Fumaric acid	6.53	(s)
Choline	3.22	(s)
Succinic acid	2.44	(s)

By comparing the data from the obtained NMR spectra –  $^1\text{H}$  and 2D (COSY, HSQC and total homonuclear correlation spectroscopy - TOCSY) with those in the literature, the presence of the secondary metabolites VER and LEU was confirmed (Figure 10).

In the  $^1\text{H}$  NMR and HSQC spectra of the extract, characteristic VER signals are observed from two ABX-type systems: signals for H-2 ( $\delta_{\text{H}}$  6.80, d/ $\delta_{\text{C}}$  118.52), H-5 ( $\delta_{\text{H}}$  6.79, d/ $\delta_{\text{C}}$  118.11) and H-6 ( $\delta_{\text{H}}$  6.69, dd/ $\delta_{\text{C}}$  124.19), corresponding to the 3,4-dihydroxy- $\beta$ -phenylethoxyl moiety and signals for H-2''' ( $\delta_{\text{H}}$  7.16, d/ $\delta_{\text{C}}$  117.17), H-5''' ( $\delta_{\text{H}}$  6.89, d/ $\delta_{\text{C}}$  118.65) and H-6''' ( $\delta_{\text{H}}$  7.08, dd/ $\delta_{\text{C}}$  121.90) for the caffeoyl residue. The doublets for the two trans-olefin protons  $\alpha'$  ( $\delta_{\text{H}}$  6.37, d/ $\delta_{\text{C}}$

*Antipsoriatic activity of plant in vitro systems, Koycheva I.K., 2025*



**Figure 10. Chemical structure of verbascoside and leucosceptoside A (A); Total correlation spectroscopy ( $^1\text{H}$ - $^1\text{H}$  TOCSY) and NMR spectra of *H. procumbens* cell suspension extract (B), the aromatic part of the spectra (C);  $^1\text{H}$ - $^1\text{H}$  homonuclear correlation spectroscopy (COSY) (D) and  $^1\text{H}$ - $^{13}\text{C}$  HSQC NMR signals (E).**

In addition, the disaccharide structure is identified by the presence of signals for the two anomeric protons H-1' ( $\delta_H$  4.49, d/ $\delta_C$  105.57) and H-1'' ( $\delta_H$  5.13, s/ $\delta_C$  104.41), corresponding to  $\beta$ -glucose and  $\alpha$ -rhamnose (Burgos et al., 2020; Santos-Cruz et al., 2012). The chemical shifts of the LEU signals were similar to those of VER, except that in the  $^1H$  and  $^{13}C$  spectra of the LEU, additional signals were observed at  $\delta_H$  3.90 (3H, s) and  $\delta_C$  60.19, respectively, corresponding to the presence of a methoxy group. Comparison of the data with those in the literature determined that the acyl moiety was ferulic acid (Youssef et al., 2017). The presence of both compounds in the extract was confirmed by the characteristic correlations observed in the  $^1H$ - $^1H$  COSY, TOCSY and HSQC spectra (Figure 10).

In the present study, 3.68 g of dry extract was obtained from 10.04 g of dry biomass of devil's claw cell suspension. The determined VER and LEU contents by HPLC (Figure 11) were approximately 4% and 1% (Table 4).

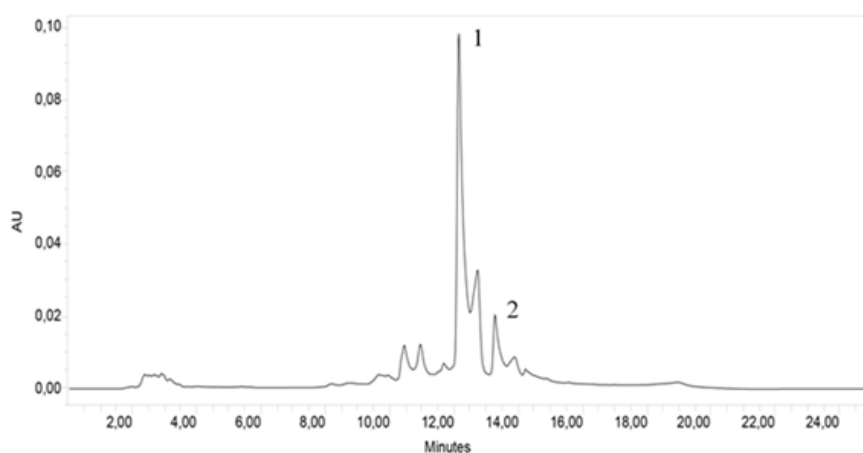


**Figure 11. HPLC chromatogram of *H. procumbens* cell suspension extract. Peaks: 1, verbascoside VER; 2, leucosceptoside A.**

**Table 4. Phenylethanoid glycosides content in *H. procumbens* (HP) cell suspension extract determined by HPLC.**

Metabolite	Retention time, (min)	Content, (mg/g)	
		HP Biomass	HP extract
Verbascoside	12.132	$10.94 \pm 1.18$	$3.99 \pm 0.49$
Leucosceptoside A	13.257	$1.64 \pm 0.16$	$0.60 \pm 0.07$

## 2.2. *In vitro* evaluation of anti-inflammatory activity of *H. procumbens*, verbascoside and leucosceptoside A in human keratinocytes

To determine non-toxic treatment concentrations, cell viability of HaCaT keratinocytes was examined (Figure 12). The 24 hours exposure of the extract, VER and LEU did not significantly affect the cell viability of HaCaT, up to 100 µg/mL for the extract and up to 100 µM for the individual pure compounds, respectively.

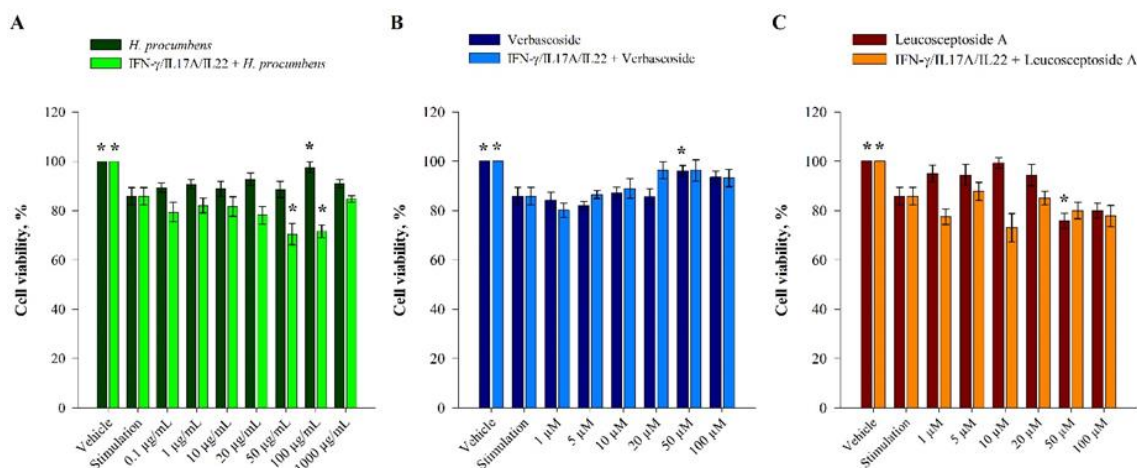


**Figure 12.** Effect of *H. procumbens* cell suspension extract (A), pure verbascoside (B) and pure leucosceptoside A (C) on cell viability of human keratinocytes. The results are expressed from three independent experiments (mean  $\pm$  SEM; \* $p$ <0.05 compared to untreated controls).

### 2.2.1. Determination of the interaction potential between the studied natural compounds and selected protein structures

The affinity of small molecule compounds for specific proteins can be predicted by docking calculations, which facilitate the elucidation of the molecular mechanisms of action of the compounds and suggest direct interactions between the studied structures and the target proteins, including van der Waals, hydrogen and pi bonds (Jin et al., 2016). The interactions of the studied compounds with the target proteins are expressed as binding free energy ( $\Delta G$ ) and affinity binding constant ( $K_i$ ; Table 5).

**Table 5.** Free energy of binding ( $\Delta G$ , kcal/M) and affinity constant ( $K_i$ ,  $\mu$ M) for each compound to protein structure.

Target protein	Verbascoside		Leucosceptoside A	
	$\Delta G$ (kcal/M)	$K_i$ ( $\mu$ M)	$\Delta G$ (kcal/M)	$K_i$ ( $\mu$ M)
AKT	-7.5	3.20	-7.2	5.40
PI3K	-9.7	0.08	-8.8	0.40
pSTAT1	-8.5	0.60	-8.2	1.00
JAK2	-7.5	3.20	-7.2	5.40

The theoretically calculated values of  $\Delta G$  and  $K_i$  suggest that the indicated proteins are among the main targets of the two compounds. A putative submicromolar affinity (0.1-5.4  $\mu M$ ) is indicated, with low  $K_i$  values suggesting a higher probability of interaction.

To predict the putative binding affinities between VER and LEU with target psoriasis-related proteins AKT; PI3K; pSTAT1 and JAK2, the molecular docking analysis approach was used (Figures 13 and 14).

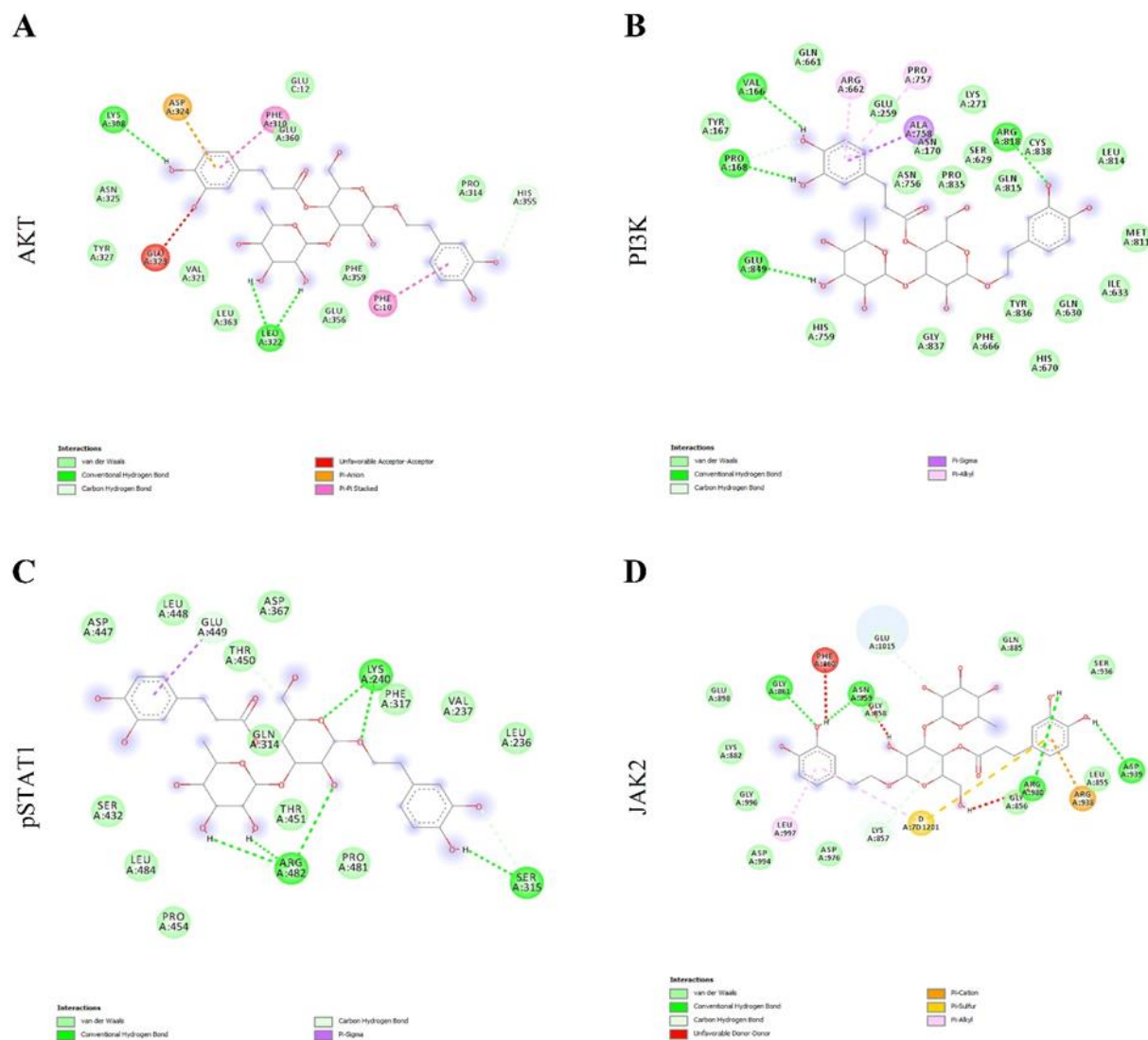


**Figure 13. Putative molecular interactions between verbascoside (VER) and AKT (A); VER and PI3K (B); VER and pSTAT1 (C); VER and JAK2 (D).**

2.2.2. *H. procumbens* cell suspension extract and its compounds verbascoside and leucosceptoside A modulate the gene expression profile of IFN- $\gamma$ /IL-17A/IL-22-stimulated keratinocytes

Inflammation plays a significant role in the development of psoriasis and therefore keratinocyte inflammation is its hallmark (Andres et al., 2013; Yang et al., 2020). The transcription factor NF-



**A**

**AKT**

**B**

**PI3K**

**C**

**pSTAT1**

**D**

**JAK2**

**Interactions**

van der Waals  
Conventional Hydrogen Bond  
Unfavorable Donor-Donor  
Pi-Alkyl  
Pi-Pi  
Pi-Sigma  
Unfavorable Acceptor-Acceptor

Inflammatory stimulation phosphorylates and degrades I $\kappa$ B *via* the I $\kappa$ B kinase (IKK) complex, leading to the release and nuclear translocation of the p65 subunit. This in turn activates the canonical NF- $\kappa$ B pathway. Activation of p65 triggers the secretion of IL-8 and CCL20 and

complicates the inflammatory response (Yang et al., 2020). The results of RT-qPCR analysis of the expression of pro-inflammatory and psoriasis-related genes showed that devil's claw extract and its secondary metabolites VER and LEU were involved in the regulation of the gene expression profile of IFN- $\gamma$ /IL-17A/IL-22-stimulated keratinocytes (Figure 15). Treatment with devil's claw extract and VER increased the expression of *CXCL8*, *PTGS2* and *CCL2*, *CCL20* through the activation of NF- $\kappa$ B, suggesting an enhancement of the immune response and aggravation of the psoriasis-like inflammatory environment by the application of the extract and that of VER. In contrast, LEU was not involved in such regulation. Inhibition of NF- $\kappa$ B and reduction of its associated downstream cytokines has been demonstrated as a mechanism of action for anti-inflammatory and antipsoriatic effects of a number of extracts, fractions, or pure compounds *in vitro* and *in vivo* (Kim et al., 2018; Balkrishna et al., 2019; Guo et al., 2021).

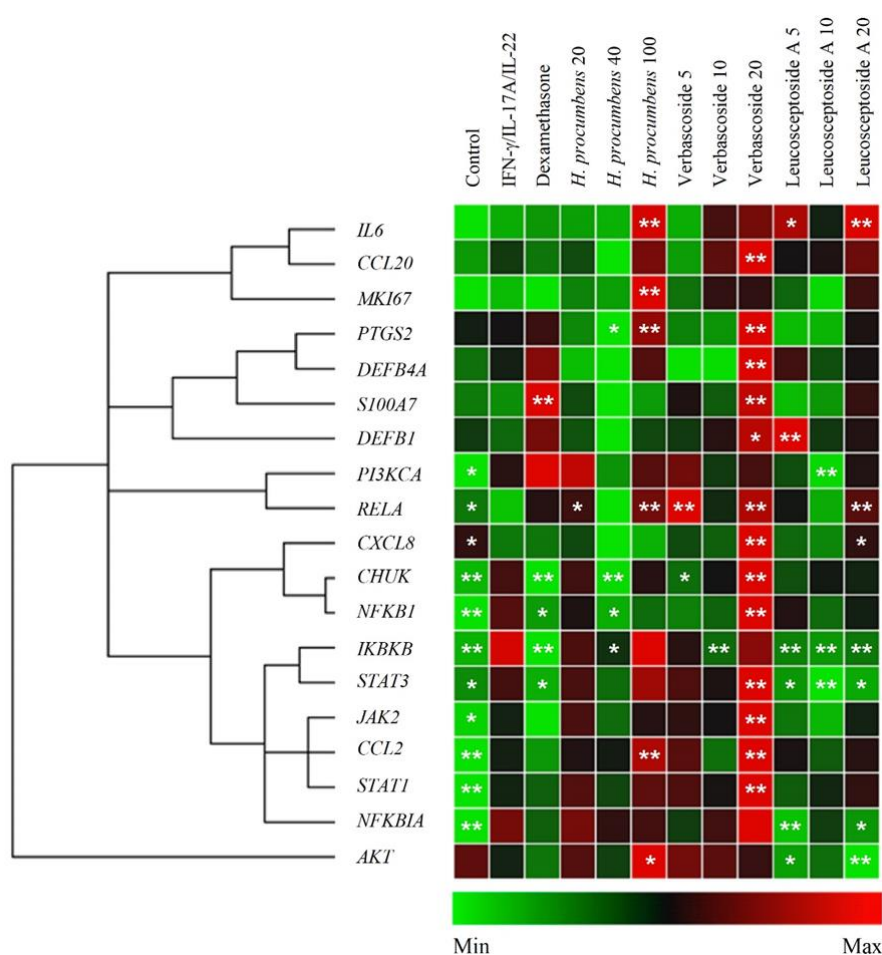


**Figure 15.** *H. procumbens* cell suspension extract and pure leukosceptoside A balance the expression of inflammation-related genes in the *in vitro* psoriasis-like model. The clustergram and heatmap of relative gene expression analysis from RT-qPCR. The representative data from three independent experiments (mean  $\pm$  SEM; \* $p$  < 0.05 and \*\* $p$  < 0.01 compared to the psoriasis model group).



In this context, the results revealed that devil's claw extract and its metabolite VER demonstrated stimulatory effects in the present model, promoting the production of pro-inflammatory mediators and keratinocyte proliferation through the activation of NF- $\kappa$ B. These findings support the hypothesis that the activity of the extract is due to the content of VER. Furthermore, VER treatment led to increased mRNA levels of psoriasis markers (*CCL20*, *S100A7*, *DEFB1*, *DEFB4A*). In this case, due to the mechanism of NF- $\kappa$ B activation and the positive expression of *CCL20* among others, the administration of VER could enhance psoriasis-related inflammation. At the same time, *CCL20* and NF- $\kappa$ B signaling were not affected by LEU treatment. Treatment with biotechnologically produced devil's claw extract at a concentration of 40  $\mu$ g/mL inhibited NF- $\kappa$ B signaling genes (*CHUK*, *IKBKB* and *NFKB1*) at the mRNA level. This was accompanied by an increase in the relative gene expression of *RELA* and *NFKBIA*. Taken together, these results indicate activation of the NF- $\kappa$ B signaling pathway and are consistent with the positive regulation of the expression of *CCL2*, *IL6* and *PTGS2* (encoding cyclooxygenase-2). Interestingly, devil's claw extract demonstrated regulation of the mRNA expression of *PTGS2* in both directions. As a result of treatment with its intermediate concentration (40  $\mu$ g/mL), *PTGS2* expression was decreased, while when treated with the highest concentration used (100  $\mu$ g/mL), it was significantly increased. At the same time, devil's claw extract at its highest concentration also increased the expressions of *MKI67* and *AKT*. This regulation was not observed with LEU. Therefore, it is suggested that the activation of NF- $\kappa$ B by the *H. procumbens* extract is due to the VER content or the total phenolic content. Interestingly, the individual pure compounds VER and LEU studied, which have similar chemical structures (Figure 10A), exhibited different biological activities in psoriatic keratinocytes. Treatment with VER at its highest concentration (20  $\mu$ M) resulted in a sharp induction of mRNA levels of almost all of the genes tested, including *CCL2*, *CCL20*, *CXCL8*, *PTGS2*, *S100A7*, beta defensin (*DEFB*)1, *DEFB4A*, *CHUK*, *RELA*, *NFKB1*, *JAK2*, *STAT1*, and *STAT3*. VER has been shown to possess anti-inflammatory properties and inhibit NF- $\kappa$ B signaling in various tissues (Georgiev et al., 2010; Gyurkovska et al., 2011). However, in the present model system, it induced a rather pro-inflammatory effect in psoriatic keratinocytes. The other phenylethanoid glycoside - LEU suppressed the mRNA expression of *IKBKB* and *NFKBIA* and increased the gene expression of *RELA* at its highest treatment concentration (20  $\mu$ M). Therefore, we can suggest that LEU rather modulates the NF- $\kappa$ B signaling pathway. JAK/STAT signaling is another transcriptional pathway involved in inflammatory and immune-mediated disorders (rheumatoid arthritis, psoriasis, and inflammatory bowel disease), and it carries out signal transduction downstream of cytokines critical for psoriasis pathogenesis (Schwartz et al., 2017; Nogueira et al., 2020). JAK/STAT activation is characteristic and highly

expressed in psoriasis disease (Banerjee et al., 2017; Schwartz et al., 2017; Nogueira et al., 2020). Anti-inflammatory activity achieved by inhibiting NF- $\kappa$ B and JAK/STAT signaling has been reported both *in vitro* and *in vivo* (Kim et al., 2014; Kim et al., 2018; Sun et al., 2019; Bian et al., 2020; Li et al., 2020). Similarly, in the present experimental data, JAK2 protein expression was upregulated, while STAT1 phosphorylation was not affected by treatment with devil's claw extract, VER, and LEU in IFN- $\gamma$ /IL-17A/IL-22-stimulated keratinocytes. These findings suggest that the studied extract and the individual pure compound VER demonstrate pro-inflammatory activity in the present psoriasis model. As a result of stimulation of HaCaT keratinocytes with IFN- $\gamma$ /IL-17A/IL-22, overexpression of *CHUK*, *IKBKB*, *NFKBIA*, *NFKB1*, *JAK2*, *STAT1*, and *STAT3* genes as inflammation-related factors was observed in the model group. These increased expression levels are in agreement with previous studies that used a similar IFN- $\gamma$ /IL-17A/IL-22-induced psoriasis model in keratinocytes (Nogales et al., 2008; Albanesi et al., 2018; Li et al., 2020). The IL-17A has been shown to upregulate keratin 17 (highly expressed in psoriatic lesions) through STAT1- and STAT3-dependent mechanisms (Shi et al., 2011). The STAT1, STAT3 and NF- $\kappa$ B are known to play key roles in the transcriptome network implicated in the mechanism of psoriasis (Sun et al., 2019; Luo et al., 2021). In psoriatic skin lesions, IFN- $\gamma$ -dependent positive transcriptional regulation of the expression of approximately 400 genes and predominant upregulation of *STAT1* was found (Albanesi et al., 2018). Similar to the data reported above (from the *L. angustifolia* extract and RA treatment experiment) upon stimulation with IFN- $\gamma$ /IL-17A/IL-22, *STAT1* was affected to a greater extent than *STAT3* in the present psoriatic model (the difference in expressions was over 10-fold). In the present experiment, *STAT3* gene expression was concentration-dependently inhibited by LEU treatment. Meanwhile, in addition to the JAK/STAT signaling pathway, the PI3K/AKT/mechanistic target of rapamycin (mTOR) signaling pathway is also involved in the development and progression of psoriasis (Goldminz et al., 2013; Kim et al., 2014; Kim et al., 2018; Li et al., 2020; Thatikonda et al., 2020). Activation of PI3K/AKT/mTOR and STAT3 signaling are known to promote acanthosis, which has been implicated in the immunopathogenesis of psoriasis (Madonna et al., 2012; Buerger et al., 2018). Chronic epidermal hyperplasia in psoriatic lesions is due to keratinocyte proliferation and key immune response events expressed by overactivation of PI3K/AKT/mTOR and STAT3 signaling (Gangadevi et al., 2021; Lu et al., 2021). Inactivation of PI3K and AKT pathways reduced proliferative effects in psoriatic keratinocytes and ameliorated psoriasis-like pathologies *in vitro* and *in vivo* (Banerjee et al., 2017; Li et al., 2019b; Xie et al., 2021b). A study by Thatikonda et al. (2020) reported a decrease in the proliferation marker Ki67 by inhibiting AKT signaling. The present study confirms that stimulation of HaCaT cells with IFN- $\gamma$ /IL-17A/IL-22 induces upregulation of PI3K/AKT-related genes and

Ki67, which is one of the important markers of hyperproliferation in psoriatic skin. The *PI3KCA* gene expression was reduced by LEU treatment, while that of *AKT* was downregulated by both VER and LEU. Therefore, it can be hypothesized that the inhibition of *AKT* signaling observed by VER and LEU treatment may lead to the downregulation of proliferation of activated HaCaT cells. However, the present results show that VER and LEU treatment did not affect the expression of the proliferation marker Ki67, maintaining its levels compared to those of the control group. However, further experiments are needed to identify the exact target site of *AKT*. Collectively, these results indicate that devil's claw extract primarily regulates NF- $\kappa$ B-related genes and their activation induces an immune response, and thus may inhibit keratinocyte hyperproliferation. The pure compound VER affected genes from both NF- $\kappa$ B and JAK/STAT signaling pathways. In addition, devil's claw extract activated *AKT* mRNA expression, while LEU suppressed those of *STAT3*, *PI3KCA*, and *AKT* in stimulated keratinocytes. The results indicate that LEU affects keratinocytes by suppressing PI3K/*AKT* signaling. Furthermore, the inhibition of overactivated *AKT* gene expression suggests that LEU may modulate the keratinocyte differentiation program in psoriasis.

### 2.2.3. Effect of *H. procumbens* extract and pure VER and LEU on the expression of key psoriasis-related proteins

To clarify the underlying molecular mechanisms of action of devil's claw extract, VER and LEU, and to complement the data from the RT-qPCR analysis, the proteins of transcription factors involved in the pathogenesis of psoriasis were investigated by immunoblot analysis.

The results of the present experiment revealed that at the protein level, JAK2, STAT1 and PI3K were activated, while *AKT* was not induced in the psoriasis model group. The data from the immunoblot analysis (Figure 16) indicated a decreased level of total STAT1 protein under the influence of devil's claw extract, VER and LEU (Figure 16B), while that of pSTAT1 was moderately affected by the treatment with LEU (Figure 16B). Compared with the results obtained from the RT-qPCR analysis (Figure 15), the gene expression level of *STAT1* was not affected by either devil's claw extract or phenylethanoid glycosides treatment. Furthermore, evaluation of JAK2 protein expression (Figure 16A) demonstrated that the extract (100  $\mu$ g/mL), LEU (10, 20  $\mu$ M) and VER (5, 10  $\mu$ M) increased its expression levels. Treatment with LEU did not affect JAK2 activation.

A highly active PI3K/*AKT*/mTORC1 pathway can lead to abnormal keratinocyte differentiation, which is generally recognized as a core pathological feature of psoriasis (Chamcheu et al., 2016; Buerger et al., 2018; Lu et al., 2021). Inactivation of PI3K/*AKT* signaling provides a

novel approach for the treatment/management of psoriasis (Zhang et al., 2021b). The classical PI3K/AKT pathway leads to activation of intracellular signaling that regulates cell metabolism, growth, proliferation, differentiation, and migration (Engelman et al., 2006; Thatikonda et al., 2020; Teng et al., 2021). Dysregulation of the PI3K/AKT/mTOR pathway has been associated with skin diseases, acne, and psoriasis. PI3K binds to AKT and in turn activates mTOR, which promotes keratinocyte hyperproliferation and inhibits their differentiation (Teng et al., 2021). The results obtained showed that the level of PI3K protein was not affected by treatment with devil's claw extract, VER or LEU (Figure 16D), while AKT was inhibited by VER (5 and 10  $\mu$ M) and LEU (20  $\mu$ M) in stimulated HaCaT cells (Figure 16E). These data confirm the inhibitory effect on AKT signaling of the compounds (especially LEU, as it also reduces gene expression), suggesting a possible PI3K-independent interaction.

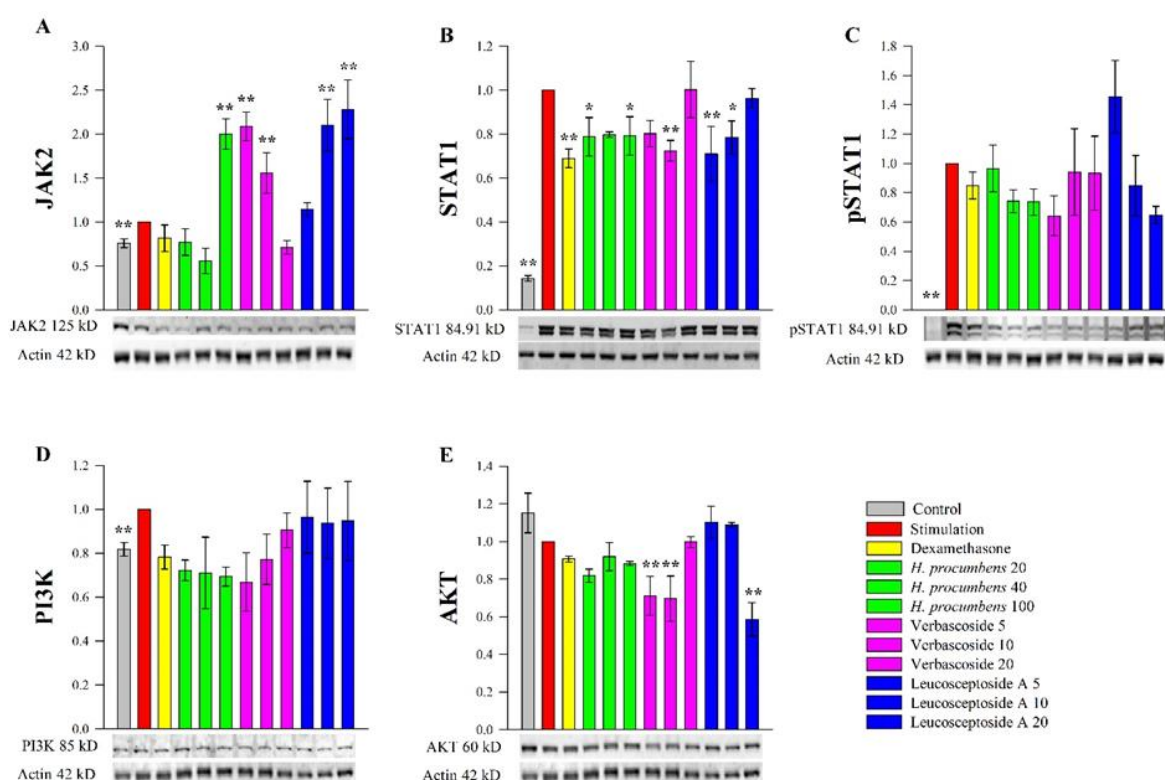


**Figure 16. Effect of *H. procumbens* extract and the individual pure compounds verbascoside and leucosceptoside A on the key psoriasis-related proteins.** Proteins expression of JAK2 (A), STAT1 (B), phosphorylated STAT1 (C), PI3K (D) and AKT (E) obtained from immunoblot analysis normalized over  $\beta$ -actin. The representative data from three independent experiments (mean  $\pm$  SEM; \* $p$  < 0.05 and \*\* $p$  < 0.01 compared to the psoriasis model group).

In summary, a molecular mechanism of biological action of devil's claw extract, VER and LEU in keratinocytes is proposed (Figure 17).

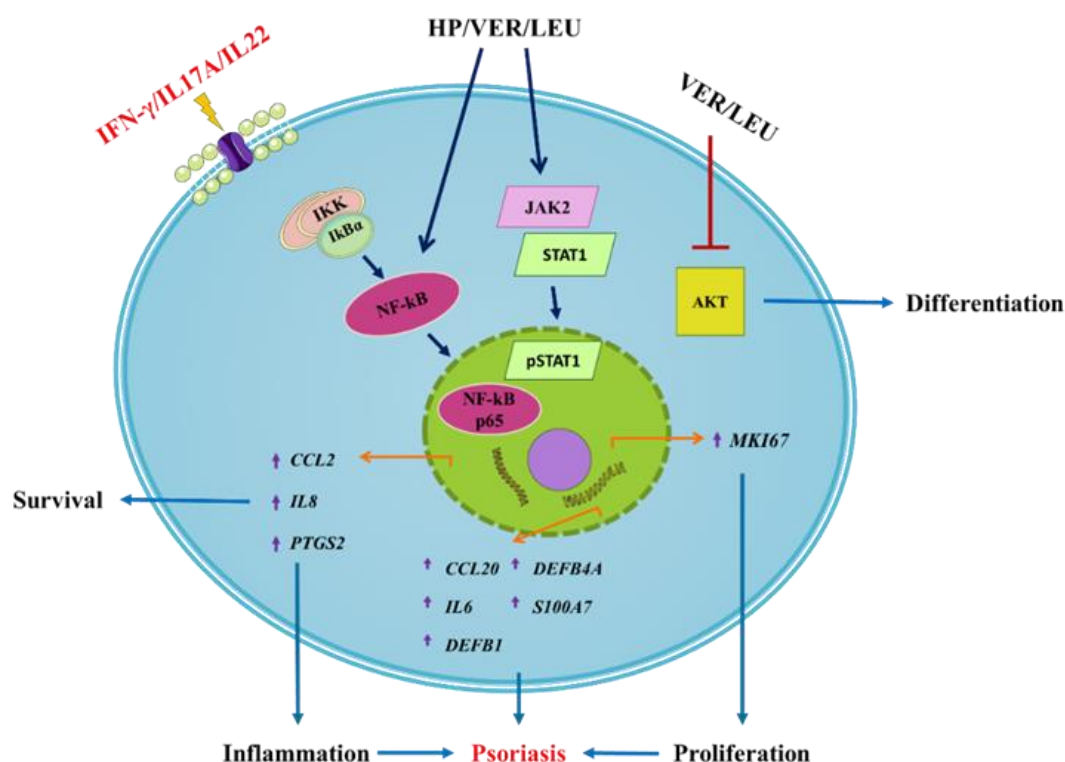


**Figure 17. Proposed mechanism of action of *H. procumbens* extract (HP), individual pure compounds verbascoside (VER) and leukoskeptoside A (LEU) on the transcriptional regulation of genes related to inflammation and psoriasis in IFN- $\gamma$ /IL-17A/IL-22-stimulated keratinocytes.** The HaCaT cells exposed to the combination of pro-inflammatory cytokines respond by activating the NF- $\kappa$ B, JAK2/STAT1 and PI3K/AKT signaling pathways. Activation of JAK2 under cytokine stimulation leads to activation of STAT1 and its subsequent phosphorylation. Following activation and nuclear translocation of NF- $\kappa$ B, phosphorylated STAT1 transcriptional activation of psoriasis-related inflammatory genes is induced in activated keratinocytes (e.g. *IL6*, *CXCL8*, *CCL20*, *CCL2*, *PTGS2*, *DEFB1*, *DEFB4A* and *S100A7*). Simultaneously, activation of the PI3K/AKT axis in psoriatic keratinocytes correlates with induction of hyperproliferation, impaired differentiation, and exacerbation of the inflammatory environment. The phenylethanoid glycosides VER and LEU interfere with psoriasis-associated inflammation by suppressing the AKT signaling.

Surprisingly, the results demonstrated that devil's claw extract and VER exhibited stimulatory rather than anti-inflammatory effects in human keratinocytes by activating NF- $\kappa$ B and JAK2/STAT1 signaling. Furthermore, it was observed that VER and LEU could inhibit AKT signaling, suggesting a potential modulation of keratinocyte proliferation and differentiation in psoriasis. Taken together, these observations indicate that biotechnologically produced devil's claw extract and the phenylethanoid compounds VER and LEU affect the JAK2/STAT1 signaling

pathway in psoriatic keratinocytes. Furthermore, at the protein level, VER and LEU could interfere with PI3K/AKT signaling.

### **3. *In vivo* validation of the anti-inflammatory effect of rosmarinic acid**

Despite the availability of various psoriasis therapies, their limitations and adverse effects continue to pose significant challenges (Zhang et al., 2021c; Zhong et al., 2022; Carmona-Rocha et al., 2024; Ferrara et al., 2024). Therefore, the development of innovative therapeutic strategies is essential (Zhang et al., 2021c; Zhong et al., 2022). In this context, natural products have emerged as promising sources of biologically active compounds with potential antipsoriatic properties (Dabholkar et al., 2020; Pinto et al., 2020; Griffiths et al., 2021; Nguyen et al., 2022; Ramanunny et al., 2022; Zhong et al., 2022). Furthermore, natural compounds are increasingly being considered as useful and safe adjuvant therapeutic options for the relief of psoriasis symptoms and have significant potential for integration into drug products (Burlec et al., 2024). More than 50% of psoriasis patients receiving conventional therapy use additional herbal and alternative products to reduce adverse reactions and relieve psoriatic skin irritations (Dabholkar et al., 2020; Du et al., 2022). The experimental approach used in the present dissertation to determine the *in vivo* antipsoriatic potential of RA involves an animal model of IMQ-induced psoriatic dermatitis in mice. Topical application of 5% IMQ, a Toll-like receptor 7/8 ligand, induces psoriasis-like dermatitis with characteristic psoriatic inflammation skin manifestations that closely resemble those of plaque psoriasis in humans (Lin et al., 2016; Gangwar et al., 2022). The effect of topical application of the cream on RA was determined by PASI score and histological analysis of skin samples.

#### **3.1. Effect of RA on the survival of spleen-isolated murine T-cells**

Psoriasis is increasingly recognized as a skin disease characterized by immune dysregulation. Its pathogenesis involves a dysregulated communication between the innate and adaptive immune responses, which is further exacerbated by systemic inflammation (Albanesi et al., 2018; Zhang et al., 2021c). Various types of immune cells with abnormal activation and interactions play a critical role in the pathogenesis of psoriasis. The T-lymphocytes are responsible for the accumulation of cytokines and chemokines in the epidermis, which promote the proliferation of epidermal keratinocytes (Girolomoni et al., 20017; Albanesi et al., 2018). In addition, the recruitment and activation of neutrophils by macrophages contributes to the differentiation and activation of T-cells, which further exacerbates the inflammatory environment (Singhet al., 2024). In this regard, several approaches have been used to comprehensively evaluate the *in vivo* antipsoriatic potential of RA. Initially, the effect of RA on T-cell proliferation isolated from the spleen of healthy mice



was assessed (Figure 18).

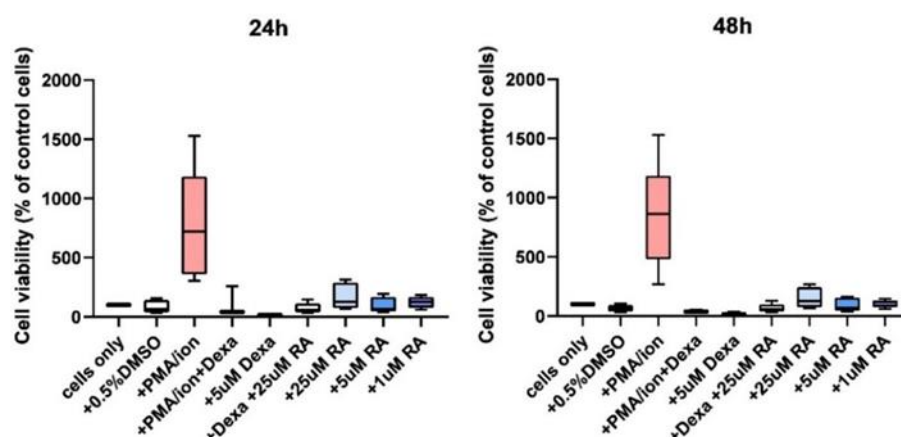


**Figure 18. Rosmarinic acid (RA) effect on cell viability of spleen-isolated murine T-cells.** Treatment with RA (25  $\mu$ M) at 24 and 48 hours did not significantly affect T-cell viability. Data are presented as percentage of control cells and were analyzed by one-way ANOVA followed by Dunnett's multiple comparison test. The representative data from three independent experiments (mean  $\pm$  standard deviation; n=4/group; \*p <0.05, \*\*p <0.01, \*\*\*p <0.005).

Data analysis showed that there was no drastic change in the percentage of the analyzed T-cell population (indicating no negative effect on lymphocytes; Figure 18). Thus, in addition to preserving their cell viability, compared to cells treated with the specific T-cell stimulus PMA, the results also illustrate the absence of nonspecific activation of T-cells as a result of RA treatment. Overall, these findings suggest that the experimental concentrations of RA treatment are safe to administer and reveal a potential anti-inflammatory effect that may be useful in alleviating local symptoms of psoriasis.

### 3.2. Topical administration of RA alleviates skin manifestations of psoriasis in mice

After confirming the hypothesis that RA does not induce a pro-inflammatory response in isolated T-cells from healthy animals, the anti-psoriatic potential of RA was further evaluated at the organism level. Already on the second day of application of IMQ cream, redness and thickening of the skin were observed, as well as a decrease in the body weight of the experimental animals. From the 4th day of treatment with IMQ cream, therapy was started with the topical formulations, which have different contents of RA (Figure 19) and a cream with betamethasone.

In the present research, IMQ application induced characteristic psoriatic histological features, including hyperkeratosis, parakeratosis in the stratum corneum, moderate acanthosis,

immune cell infiltration in the dermis, and skin inflammation, consistent with findings in the literature (van der Fits et al., 2009; Chen et al., 2020; Choi et al., 2021; Jin et al., 2021; Gangwar et al., 2022; Rai et al., 2022; Xiang et al., 2022; Köhler et al., 2024).

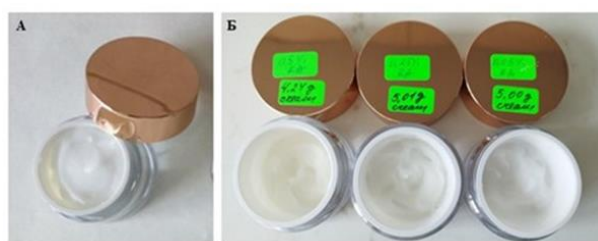


**Figure 19. Cream containing rosmarinic acid (RA). (A) 0% RA; (B) 0.05, 0.25, 0.50 % RA.**

In the present research, IMQ application induced characteristic psoriatic histological features, including hyperkeratosis, parakeratosis in the stratum corneum, moderate acanthosis, immune cell infiltration in the dermis, and skin inflammation, consistent with findings in the literature (van der Fits et al., 2009; Chen et al., 2020; Choi et al., 2021; Jin et al., 2021; Gangwar et al., 2022; Rai et al., 2022; Xiang et al., 2022; Köhler et al., 2024). Histological evaluation of skin samples from the control group of animals showed a normal, thin epidermis without inflammatory cell infiltration. Meanwhile, analysis of skin samples from animals with IMQ-induced psoriasiform dermatitis revealed infiltration of lymphoid and polymorphonuclear cells (red arrows) in the dermis, significant epidermal hyperplasia (orange arrows) and hyperkeratosis (blue arrows), observed six days after the induction of psoriatic inflammation (Figure 20).

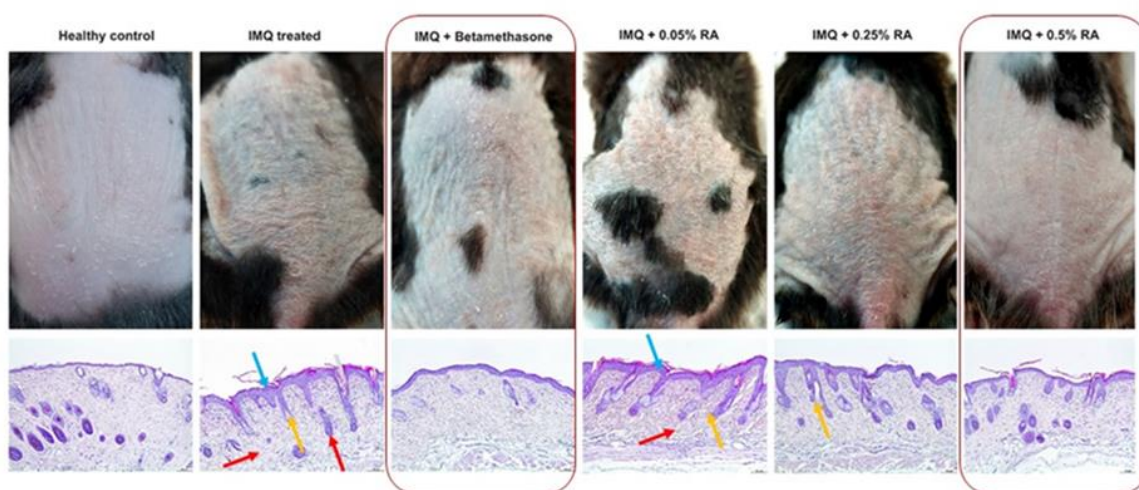


**Figure 20. Histological evaluation of skin samples from animals with imiquimod (IMQ)-induced psoriasiform dermatitis treated with rosmarinic acid (RA; 0, 0.05, 0.25 and 0.50%) and betamethasone (0.05%).** Representative images of animals from all experimental groups, captured under a light microscope at 10x magnification, as follows: healthy control (control), model



group (IMQ), IMQ+Betamethasone, IMQ+RA. Skin sections were stained with hematoxylin/eosin. Red arrows indicate infiltration of lymphoid and polymorphonuclear cells in the dermis; orange arrows highlight significant epidermal hyperplasia, and blue arrows indicate hyperkeratosis.

At the same time, as a result of the application of RA, a decrease in the degree of cellular infiltration in the dermis was recorded (of lymphoid and polymorphonuclear cells; Figure 20), which is associated with reduced cytokine production and a general decrease in inflammation (Li et al., 2016). Additionally, during the observation, an improvement in the skin condition was noted, alleviating hyperkeratosis in the animals in the RA-treated groups, compared to the control animals (Figure 20). The results of the analysis of histological sections and the values of the skin thickness measurements clearly illustrate the achievement of the psoriatic model *in vivo* and the effect of RA treatment (Figures 20 and 21).

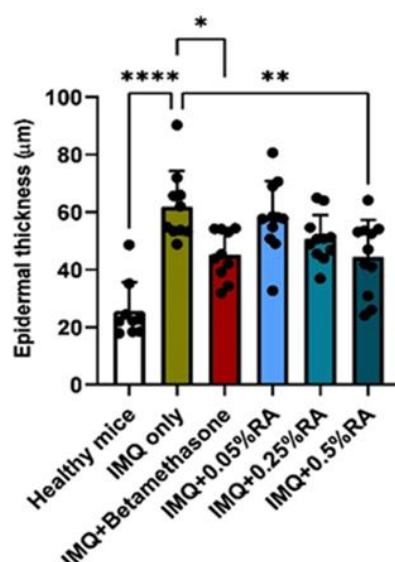


**Figure 21. Rosmarinic acid (RA) reduces epidermal thickening in imiquimod (IMQ)-induced psoriasiform dermatitis in C57BL/6 mice.** Graphical representation of epidermal thickness (μm). Data were analyzed by one-way ANOVA followed by Dunnett's multiple comparison test. The representative data from three independent experiments (mean ± standard deviation; n=4/group; \*p <0.05, \*\*p <0.01, \*\*\*p <0.005, \*\*\*\*p <0.001).

Furthermore, the highest concentration of topical RA (0.5%) resulted in significant skin repair and a reduction in one of the hallmarks of psoriasis, epidermal hyperplasia (thickening of the epidermis), compared to healthy controls, to levels comparable to those treated with the positive control (betamethasone; Figures 20 and 21). This result is consistent with studies that have shown the effectiveness of topical treatments such as acarbose and cyclosporine A in an IMQ-induced

model of psoriasis (Chen et al., 2020). The administration of piperlongumine, included in the composition of 0.75% gel at doses of 10 and 30 mg/kg (compared to ointment containing 20 mg/kg tacrolimus), attenuated IMQ-induced parakeratosis and epidermal acanthosis, and significantly reduced ear thickness in piperlongumine-treated groups of mice (Thatikonda et al., 2020). Additionally, the severity of induced psoriatic dermatitis and the therapeutic outcome of RA application were determined using the PASI index (Figure 22). A decrease in PASI of at least 50% is considered a significant improvement in psoriasis (van der Fits et al., 2009; Chen et al., 2020; Rai et al., 2022; Xiang et al., 2022). According to this criterion, therapy with 0.5% RA resulted in an approximately 50% decrease in PASI values. The cumulative PASI score obtained in the present model indicates that topical RA application significantly alleviates the symptoms of IMQ-induced psoriatic dermatitis, such as erythema, scaling, and thickness of the skin lesions (Figure 22).

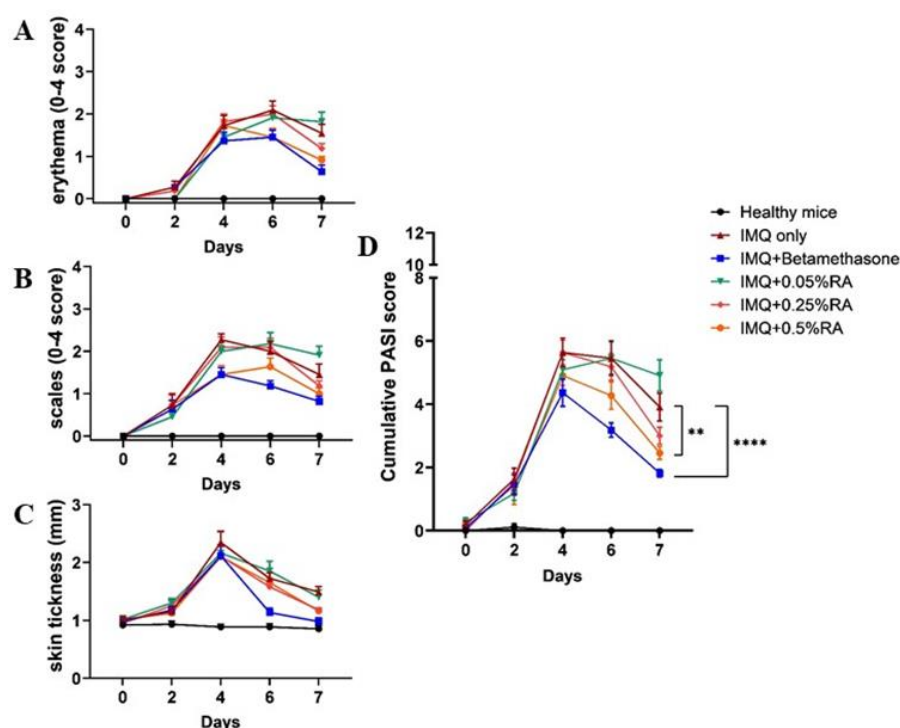


**Figure 22. Effect of rosmarinic acid (RA) in imiquimod (IMQ)-induced psoriasiform dermatitis in mice.** Presentation of (A-C) adapted PASI index (0-4), taking into account the degree of redness, scaling, skin thickness and skin lesions; (D) cumulative PASI index. Data were analyzed by one-way ANOVA test followed by Tukey's multiple comparison test. The representative data from three independent experiments (mean  $\pm$  standard deviation;  $n=4$ ; \* $p < 0.05$ , \*\* $p < 0.01$ , \*\*\* $p < 0.005$ , \*\*\*\* $p < 0.001$ ).

The results obtained are consistent with data from previous studies evaluating the topical application of various individual compounds such as acarbose, cyclosporine A, anoctamine-1,

allantolactone, linalool, and tetrandrine. These substances have shown efficacy in alleviating IMQ-induced skin lesions in a mouse model of psoriasiform dermatitis (Chen et al., 2020; Thatikonda et al., 2020; Choi et al., 2021; Jin et al., 2021; Chen et al., 2022; Rai et al., 2022; Li et al., 2023). Other experimental results, again on an IMQ-induced mouse model of psoriasis, have demonstrated a significant reduction in: scaling, erythema, and skin thickening, accompanied by downregulation of IL-17A, Ki67, and CD4<sup>+</sup> T-cell expressions after topical application of an indirubin-loaded microemulsion gel (He et al., 2022).

### 3.3. Effects of topical RA application in an *in vivo* model of psoriatic inflammation

A biological endpoint, such as a systemic inflammatory response occurring in both the spleen and lymph nodes, is widely used to study therapeutic efficacy in psoriasis *in vivo* (Jabeen et al., 2020; Li et al., 2023). Data for such an assessment in the present experiment are presented in Figure 23.

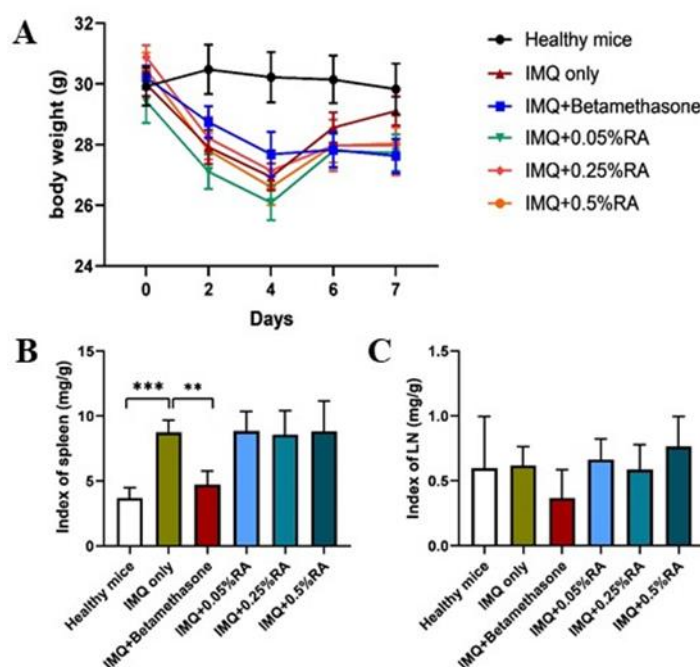


**Figure 23. Effect of rosmarinic acid (RA) in imiquimod (IMQ)-induced psoriasiform dermatitis in mice.** Presentation of (A) body weight of the experimental animals during psoriasis modelling and treatment, representation of (B) spleen index and (C) lymph node index, calculated according the body weight of the animals. Data were analyzed by one-way ANOVA test followed by Dunnett's multiple comparison test. The representative data from three independent experiments (mean  $\pm$  standard deviation; n=4/group; \*p < 0.05, \*\*p < 0.01, \*\*\*p < 0.005).

In the study, without body weight reduction effect was observed in the RA-treated groups compared to the IMQ-treated groups alone. A significant reduction in spleen weight was reported

in the betamethasone-treated animals. Compared to the control groups, the results showing no systemic effects on animal weight, spleen size, and lymph node size confirm primarily a local effect at the site of application of the RA emulsion. In summary, the present study highlights the potential therapeutic role of RA-containing emulsions in alleviating the cutaneous symptoms of psoriasis. The results obtained demonstrate that RA effectively inhibits the progression of IMQ-induced psoriasiform dermatitis in mice and reduces the formation of psoriatic lesions, supporting the conclusions regarding the potential of RA as a therapeutic agent for the control of psoriasis. These results contribute to the growing interest in the use of natural compounds with anti-inflammatory activity in dermatological therapy.

#### 4. Conclusion and future perspectives

The present dissertation includes effective application of NMR and HPLC for metabolic profiling of biotechnologically obtained extracts from cell suspensions of *L. angustifolia* and *H. procumbens*. In the analyzed extracts, plant secondary metabolites RA, VER and LEU were identified and quantified. Moreover, the anti-inflammatory activity of the extracts and their main individual compounds were studied, using modern "omics" approaches in an *in vitro* psoriasis model based on IFN- $\gamma$ /IL-17A/IL-22-stimulated human keratinocytes HaCaT. The underlying molecular mechanisms of their action were also investigated and potential mechanisms of their antipsoriatic activity were proposed. The RT-qPCR and immunoblot analyses revealed that *L. angustifolia* extract and RA inhibited JAK2/STAT1 signaling. *L. angustifolia* extract also showed inhibition of PI3K and AKT kinases, which was associated with reduced keratinocyte hyperproliferation. Separately, unlike VER and devil's claw extract, LEU ameliorated psoriasis-like inflammation by suppressing PI3K/AKT signaling in IFN- $\gamma$ /IL-17A/IL-22-induced HaCaT cells. The obtained results indicate that LEU may have therapeutic potential in psoriasis by regulating epidermal differentiation through inhibition of the AKT pathway.

The analysis of the data revealed RA as a compound with the most significant anti-inflammatory and antipsoriatic effects, respectively, in the conducted *in vitro* experiments. The proposed mechanism of RA action is associated with the inhibition of inflammatory signaling pathways. The therapeutic activity of RA has been validated using the well-established *in vivo* model of IMQ-induced psoriasiform dermatitis in C57BL/6 mice, in which topical application of RA significantly alleviates the phenotypic and histopathological manifestations of psoriatic inflammation. Despite the achieved results, the present study is limited to a preclinical model. Additional clinical studies are needed to confirm the safety, optimal dosage and long-term efficacy of RA for the treatment of psoriasis in humans.

## V. CONCLUSIONS

1. Phytochemical profile data of cell suspensions extracts from *L. angustifolia* and *H. procumbens* have been obtained.
2. The content of the secondary metabolites rosmarinic acid, verbascoside and leucosceptoside A in the studied plant extracts has been quantitatively determined.
3. Two models of psoriasis have been successfully adapted and applied: an *in vitro* model of psoriasis in human epidermal keratinocytes (HaCaT) and an *in vivo* model of psoriasiform dermatitis in mice (C57BL/6).
4. The *L. angustifolia* cell suspension extract suppresses psoriatic inflammation in human keratinocytes through inhibition of the JAK2/STAT1 signaling pathway.
5. Leucosceptoside A isolated from *H. procumbens* cell suspension extract ameliorates psoriasis-induced inflammation by suppressing PI3K/AKT signaling in IFN- $\gamma$ /IL-17A/IL-22-activated HaCaT cells.
6. Biotechnologically derived *L. angustifolia* extract, as well as the individual pure compounds rosmarinic acid and leucosceptoside A, demonstrate potential to be incorporated into topical formulations that can be used as a novel therapeutic approach to alleviate the skin manifestations of psoriasis.
7. Topical application of rosmarinic acid alleviates cutaneous symptoms of imiquimod-induced psoriatic inflammation at the organismal level.

## VI. CONTRIBUTIONS

*With scientific and fundamental character:*

1. The antipsoriatic activity of *L. angustifolia* extract, as well as rosmarinic acid and leucosceptoside A, has been established in an *in vitro* model of psoriasis in human epidermal keratinocytes (HaCaT).
2. Key molecular signaling pathways involved in the mechanism of antipsoriatic action of *L. angustifolia*, rosmarinic acid and leucosceptoside A in HaCaT cells have been identified.

*With scientific and applied character:*

1. An *in vitro* model of psoriasis was introduced and optimized, applicable as a screening platform for assessing the antipsoriatic potential of plant extracts and natural compounds.
2. An *in vivo* model of psoriasis was adapted to study the phenotypic manifestation of skin inflammation in C57BL/6 mice, which may serve as a platform for preclinical evaluation of the antipsoriatic potential of compounds of different origins, medicinal or cosmetic formulations for skin application.
3. The obtained data on the molecular mechanisms of action of *L. angustifolia*, rosmarinic acid and leucosceptoside A can serve as a scientific basis for the development of effective therapeutic agents aimed at alleviating the skin manifestations of psoriasis.
4. The potential of rosmarinic acid as an active ingredient for inclusion in topical formulations, offering a new therapeutic approach for psoriasis treatment, has been established.

## Acknowledgements

I am grateful to my supervisor Prof. Dr. Milen Georgiev for the opportunity to work on a contemporary and interesting topic, for the professional guidance, supervision and organization of this dissertation.

I Sincerely thank to my colleagues from the Metabolomics Laboratory at the Institute of Microbiology “Stephan Angeloff” – BAS, for their support, with special gratitude to Assoc. Prof. Dr. Liliya Mihaylova for her valuable guidance. I would like to thank Assoc. Prof. Dr. Nikolina Mihaylova from the Department of Immunology at the Institute of Microbiology “Stephan Angelff” – BAS, for the joint work on the adaptation of an *in vivo* model of psoriasis and experimental work on the *in vivo* experiments presented in the dissertation, as well as Assoc. Prof. Dr. Kalina Alipieva, Institute of Organic Chemistry with the Center for Phytochemistry – BAS, for the joint work on the phytochemical analysis of the studied extracts. I am grateful to Assoc. Prof. Dr. Andrey Marchev from the Department of Biotechnology at the Institute of Microbiology “Stephan Angeloff” – BAS for the assistance in the analysis of the obtained NMR spectra. I highly appreciate the cooperation of Prof. Dr. Gustino Orlando and Assoc. Prof. Dr. Claudio Ferrante from G. D'Annunzio University, Chieti, Italy, in the molecular docking analysis of the studied compounds.

I express my gratitude to the management of the Stephan Angeloff Institute of Microbiology – BAS for their institutional support and the created conditions for conducting scientific research, as well as to the management of the Center for Plant Systems Biology and Biotechnology, Plovdiv for the provided access to high-tech equipment.

I sincerely thank my family and loved ones for their invaluable support, their faith in me and the patience shown throughout the process of developing and summarizing this dissertation work.

The scientific research included in this dissertation has been carried out with financial support of the PlantaSYST project (SGA No. 739582 and FPA No. 664620) part of the Horizon 2020 program of the European Union, as well as project BG05M2OP001-1.003-001-C01, funded by the European Regional Development Fund through the operational program "Science and Education for Smart Growth" with contract No.: KP-06-H51/14 funded by the Scientific Research Fund.



## Published materials on the dissertation

### Scientific publications

1. **Koycheva I.K.**, Marchev A.S., Stoykova I.D., Georgiev M.I. (2025) Natural alternatives targeting psoriasis pathology and key signaling pathways: A focus on phytochemicals. *Phytochemistry Reviews*, 24: 2147-2173 (**IF<sub>2024</sub> 7.6; Q1**).
2. Perra M., Fancello L., Castangia I., Allaw M., Escribano-Ferrer E., Peris J.E., Usach I., Manca M.L., **Koycheva I.K.**, Georgiev M.I., Manconi M. (2022) Formulation and testing of antioxidant and protective effect of hyalurosomes loading extract rich in rosmarinic acid biotechnologically produced from *Lavandula angustifolia* Miller. *Molecules*, 27(8): 2423 (**IF<sub>2022</sub> 4.6; Q2**).
3. **Koycheva I.K.**, Vasileva L.V., Amirova K.M., Marchev A.S., Balcheva-Sivenova Z.P., Georgiev M.I. (2021) Biotechnologically produced *Lavandula angustifolia* Mill. extract rich in rosmarinic acid resolves psoriasis-related inflammation through Janus kinase/signal transducer and activator of transcription signaling. *Frontiers in Pharmacology*, 12: 680168 (**IF<sub>2021</sub> 5.988; Q1**).
4. **Koycheva I.K.**, Mihaylova L.V., Todorova M.N., Balcheva-Sivenova Z.P., Alipieva K., Ferrante C., Orlando G., Georgiev M.I. (2021) Leucosceptoside A from Devil's claw modulates psoriasis-like inflammation *via* suppression of the PI3K/AKT signaling pathway in keratinocytes. *Molecules*, 26(22): 7014 (**IF<sub>2021</sub> 4.927; Q2**).
5. Marchev A.S., Vasileva L.V., Amirova K.M., Savova M.C., **Koycheva I.K.**, Balcheva-Sivenova Z.P., Vasileva S.M., Georgiev M.I. (2021) Rosmarinic acid - from bench to valuable applications in food industry. *Trends in Food Science and Technology*, 117: 182-193 (**IF<sub>2021</sub> 16.002; Q1**).

**Total impact factor (IF): 39.1**

### Participation in scientific conferences

#### Oral reports

1. Georgiev M.I., **Koycheva I.K.** (2023) Anti-psoriatic potential of plant natural compounds. *The 9<sup>th</sup> International Mediterranean Symposium on Medicinal and Aromatic Plants*, 03-05 May, Ankara, Turkiye, Keynote lecture.
2. Georgiev M.I., **Koycheva I.K.** (2023) The anti-psoriatic potential of natural compounds. *The 7<sup>th</sup> International Symposium on Phytochemicals in Medicine and Food (7-ISPMF)*, 02-06 August, Guangzhou, China, Plenary lecture.

*Poster presentations*

1. **Koycheva I.K.**, Todorova M.N., Amirova K.M., Balcheva-Sivenova Z.P., Marchev A.S., Vasileva L.V., Georgiev M.I. (2021) *In vitro* therapeutic effects of *Lavandula angustifolia* extract and rosmarinic acid on psoriasis dermatitis. *The 1<sup>st</sup> International Conference on Plant Systems Biology and Biotechnology*, 14-17 June, Golden Sands Resort, Bulgaria, PP. 18.
2. **Koycheva I.K.**, Todorova M.N., Stoykova I.D., Balcheva-Sivenova Z.P., Vasileva L.V., Georgiev M.I. (2021) *Harpagophytum procumbens* exerts potential in psoriasis managment. *The 1<sup>st</sup> International Conference on Plant Systems Biology and Biotechnology*, 14-17 June, Golden Sands Resort, Bulgaria, PP. 46.